TAMPEREEN TEKNILLINEN YLIOPISTO
TAMPERE UNIVERSITY OF TECHNOLOGY

OLLI TIAINEN

PERFORMANCE SIMULATIONS OF A HYDRAULIC-MECHANICAL DAMPER FOR A STEERABLE THRUSTER

Master of Science thesis

Examiner: Prof. Kalevi Huhtala
Examiner and topic approved by the
Faculty Council of the Faculty of
Engineering sciences
on 9th November 2016

ABSTRACT

OLLI TIAINEN: Performance simulations of a hydraulic-mechanical damper for a steerable thruster
Tampere University of Technology
Master of Science thesis, 63 pages, 3 Appendix pages
May 2017
Master's Degree Programme in Automation Technology
Major: Hydraulics and Automation, Factory Automation
Examiner: Prof. Kalevi Huhtala
Keywords: Thruster, Damper, Ice impact

This master's thesis consists of designing and modelling a damper system for a Wärtsilä Steerable Thruster. Aim is to reduce torque peaks caused by ice impacts on the propeller shaft of the thruster. A passive ideal damper as well as a novel hydraulic-mechanical damper are modelled and the effects of the damper are simulated in varied ice impact scenarios.

Simulated ice impact cases are generated to be similar to the ones of Det Norske Veritas regulations. In addition further custom ice impacts with variable sinusoidal impact lengths are generated. Simulations are conducted without a damper, with a passive ideal damper and with the novel hydraulic-mechanical damper. A validated simulation model of the WST-14 propulsion system is given for use in this master's thesis by Tampere University of Technology Laboratory of Automation and Hydraulics.

Novel hydraulic-mechanical damper is a rotating dual-mass torsional damper. Damper consists of two main inertias; a damper case and a damper wheel, as well as hydraulic spring and damping elements. Both active and semi-active variations of the damper are considered.

Simulation results of the hydraulic-mechanical damper are studied and it is acknowledged that the damper has reasonable effect on reducing torque peaks on some impact cases and negligible or even inverse effects on certain impact cases. Most significant results of the hydraulic-mechanical damper are torque peak reduction of 8.6 % in the propeller shaft and maximum peak-to-peak reduction of over 40 %. In certain ice impact cases the simulation results show a falling torque peak reduction of maximum of 9 kNm, or over 15 % of the falling torque, resulting in prevention of gear hammering.

TIIVISTELMÄ

OLLI TIAINEN: Ohjauspotkurille tarkoitetun hydraulismekaanisen vääntövärähtelynvaimentimen mallinnus ja simulointi
Tampereen teknillinen yliopisto
Diplomityö, 63 sivua, 3 liitesivua
Toukokuu 2017
Automaatiotekniikan koulutusohjelma
Pääaine: Hydrauliikka ja Automatiikka, Koneautomaatio
Tarkastajat: Prof. Kalevi Huhtala
Avainsanat: ohjauspotkuri, vääntövärähtelynvaimennin, jääisku

Tämä diplomityö koostuu vääntövärähtelyn vaimentimen suunnittelusta ja mallinnuksesta Wärtsilän ohjauspotkurille. Työn tavoitteena on vähentää ohjauspotkurin lapoihin kohdistuvia vääntömomenttipiikkejä. Vääntömomenttipiikit aiheutuvat usein potkurin lapojen ja jäälohkareiden kontakteista. Ensin työssä mallinnetaan passiivinen ja ideaalinen vaimennin ja tämän jälkeen suunnitellaan sekä mallinnetaan pyörivä hydraulismekaaninen vaimennin. Lopulta vaimentimien toimintaa ja tehokkuutta simuloidaan ja tarkastellaan erilaisissa jääimpaktisarjoissa.

Simuloidut jääimpaktit ovat mallinnettu vastaavaan Det Norske Veritaksen säädöksistä löytyviä jääimpaktisarjoja. Työssä simuloidaan lisäksi myös eri mittaisia kustomoituja jääimpaktisarjoja. Simulaatiotarkastelut suoritetaan erilaisilla jääimpakteilla ilman vääntövärähtelyn vaimenninta, passiivisen ja ideaalisen vaimentimen kanssa sekä suunnitellun hydraulismekaanisen vaimentimen kanssa. Työssä on käytetty Tampereen teknillisen yliopiston Automaation ja hydrauliikan laboratorion suunnittelemaa ja validoimaa WST-14 ohjauspotkurin simulaatiomallia.

Suunniteltu hydraulismekaaninen vaimennin on kaksimassainen vaimennin, joka koostuu kahdesta inertiapyörästä ja hydraulisista jousi- ja vaimennuselementeistä. Vaimentimesta tutkitaan sekä aktiivista että puoliaktiivista versiota.

Hydraulismekaanisen vaimentimen simulaatiotuloksista voidaan päätellä, että vaimennin toimii joissain tapauksissa kohtuullisesti, mutta tietyissä tapauksissa vaimennin voi jopa kasvattaa vääntömomenttipiikkejä vähäisesti. Parhaat simulaatiotulokset osoittavat että vaimennin voi vähentää potkuriakselin suurimpia vääntömomenttipiikkejä 8.6 %. Parhaimmillaan vaimennin myös vähentää vääntömomentin huipusta huippuun värähtelyä 40 %. Laskevia vääntömomenttipiikkejä vaimennin pystyy simulaatioiden mukaan vähentämään maksimissaan 9 kNm, tai yli 15 %.

PREFACE

This master's thesis was carried out under the Maritime Technologies II Research Programme in the framework of the ERA-NET MARTEC II project CA 266111 ArTEco "Arctic Thruster Ecosystem". Studies were conducted in the Laboratory of Automation and Hydraulics, Tampere University of Technology.

I would like to thank my mentor Lauri Siivonen and examiner prof. Kalevi Huhtala for both the opportunity to write my thesis for this project as well as for extraordinary guidance and help during the time I have worked on my thesis. I would also like to thank Wärtsilä, VTT and all the parties of ArTEco project for making it possible for me to work on a project with an interesting topic.

Lastly I would like to thank my family and friends for all the help and support during my studies.

Tampere, 23.5.2017

Olli Tiainen

CONTENTS

LIST OF FIGURES

LIST OF ABBREVIATIONS AND SYMBOLS

AUT	Laboratory of Automation and Hydraulics
DNV	Det Norske Veritas, classification society
LGB	Lower gearbox of a thruster
TUT	Tampere University of Technology
UGB	Upper gearbox of a thruster
WST	Wärtsilä Steerable Thruster

b	Viscous friction coefficient
B	Bulk modulus of compressing oil
B_{eff}	Effective bulk modulus of a chamber
C	Damping coefficient
C_c	Critical damping coefficient
C_q	Relation of ice impact induced torque and system's nominal torque
D_o	Outer diameter of damper case/wheel
D_i	Inner diameter of damper case
F	Force
F_C	Coulombian friction force
F_S	Static friction force
F_μ	Friction force
H	Number of hydraulic elements
I_1	Inertia of damper case
I_2	Inertia of damper wheel
K	Spring coefficient
K_L	Laminar leakage coefficient
L	Length of a hollow cylinder
M	Resultant moment acting on rigid body
p_A	Pressure in chamber A
$p_{A,act}$	Pressure of auxiliary chamber A
p_{init}	Initial chamber pressure
Δp	Pressure difference over valve
Q	Fluid flow rate
T	Torque
u	Valve opening
v	Piston velocity
v_S	Velocity of minimum friction force
V	Chamber volume

V_{init}	Initial chamber volume
x	Piston displacement
Z	Number of propeller blades
α	Duration of propeller blade's impact with ice in degrees
γ	Velocity dependency factor of spring element
ζ	Damping factor
θ	Angular displacement
$\dot{\theta}$	Angular velocity
$\ddot{\theta}$	Angular acceleration
μ	Flow coefficient of valve orifice
ρ	Density of material
υ	Rotational speed of a propeller shaft

1. INTRODUCTION

Thrusters in marine vessels are used in maneuvering the ship, station keeping and dynamic positioning. Steerable thrusters such as Wärtsilä Steerable Thruster (WST) is a 360° rotatable around its Z-axis and this allows the thruster to be used effectively in maneuvering. Steerable thrusters are commonly used and intended for ships that require high maneuverability and ship station keeping such as tug boats and offshore support vessels.

Steerable thrusters are manufactured in different sizes and power levels for use in different situations. Power levels range from roughly 150 kW to well over 4 MW with different designs and manufacturers. Propeller diameters of thrusters range from under 750 mm to over 4000 mm and torque levels of thrusters range from few kilonewton meters to hundreds of kilonewton meters. [28][1]

Steerable thruster are divided into two groups of L-drive and Z-drive thrusters. L-drive thrusters have a vertical input shaft and horizontal output shaft with one gear system in between. Z-drives such as WST has horizontal input shaft, vertical shaft and horizontal output shaft with two gears in between, upper gearbox (UGB) and lower gearbox (LGB).

As thrusters are often used in ice going vessels, propeller blade impacts with ice blocks are common occurrences. Ice impacts cause torque peaks in the propeller blades and in the horizontal output shaft – the propeller shaft. Torque peaks are especially harmful for the lower gearbox and thus must be taken into account when designing the thruster and LGB. In ice impact scenarios gear failures may occur and to prevent breaking of a gear a damper system can be implemented into the thruster.

Location of a damper system is usually behind the engine or in the engine shaft. As the aim is to reduce torque peaks in the propeller shaft, a damper should be installed closer to the actual propeller shaft. Location in the propeller shaft is difficult as the damper can't be easily maintained and repaired in a case of a breakage. This leads to the fact that the damper should be maintenance free and in a case of a

malfunction or a breakage damper system shouldn't hinder the normal operations of the thruster. Possible damper systems for a propeller shaft of a steerable thruster are rotating dual-mass torsional dampers, fluid couplings and motor systems that brake or boost the propeller shaft.

The aim of this master's thesis is a reduction of ice impact induced torque peaks in a WST-14's propeller shaft. The first chapter of this thesis introduces the scope of the work, ice impacts and their effects as well as common damping methods. Rotating torsional damper is chosen as the method to reduce the torque peaks. Next the theoretical background and commercial rotating torsional dampers are studied. After the literature review in the chapter three a rotating torsional damper is designed and modelled. In the fourth chapter the modelled damper's effects are simulated and analyzed in different ice impact scenarios. Two different rotating torsional dampers are modelled; a passive ideal damper and a hydraulic-mechanical damper. Fifth and the last chapter sums up the conclusions of the thesis and discusses future research options.

2. SCOPE OF WORK AND THEORETICAL STUDIES

Scope of the thesis is to design and model a rotating torsional damper to reduce torque peaks on a propeller shaft according to requirements set by both the ArTEco project and the WST-14. One aim of the project is to reduce torque peaks caused by ice impacts by 30 % and the rotating torsional damper is one of the parts researched in order to achieve best possible torque reduction.

Limits for the damper result from the WST-14 system's physical attributes such as size, torque, location and power. The system to be damped is a high-power system with powers over 100 kW. Estimated range in the engine powers is 2-3 MW. The location of the modelled rotating torsional damper is inside the thruster in the free end of the propeller shaft. Location of the damper inside the thruster limits the damper in two significant ways; the physical size is limited as the damper must fit inside the thruster cone and also the location limits the maintenance and fault tolerance of the damper. Cone is considered the location in the back end of the propeller shaft; opposite to the propeller. Damper should be maintenance free and in case of a breakdown it should not hinder the normal operation of the thruster. Wärtsilä's Steerable Thruster-14 can be seen in Figure 2.1.

Common thruster and propeller torques range from near zero to well over 500 kNm. With WST-14 the nominal torques are considered approximately 40 kNm and this leads to dynamic torque ranges from zero to slightly over 100 kNm in this project. Small oscillation in the torque is for example caused by the shape of the propeller blades and vibrations caused by the engine. Torque peaks are caused by the thruster blades hitting ice or other obstacles. In the scope of this thesis only the torque peaks caused by ice impacts and their reduction is considered. Ice impacts and their torque responses on propeller shaft are studied and simulated with modelled dampers. Designing CAD models and a fully manufacturable damper is not in the scope of this thesis, but rather the concept and viability of the damper.

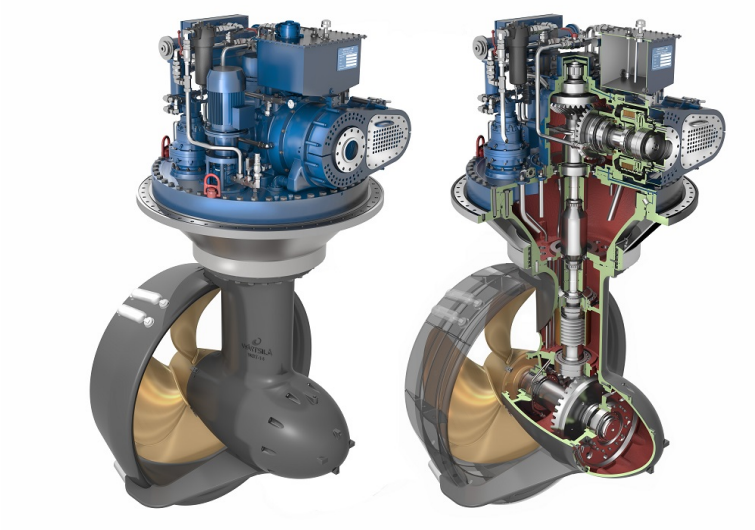

Figure 2.1. *Wärtsilä Steerable Thruster-14 [27]*

2.1 Effects of ice impacts on a propulsion system

This section studies the torsional influence on arctic vessel's propulsion system caused by the propeller blades' contacts with ice blocks. There are regulations and rules for classification of ships and the propulsion systems regarding ice impacts by Trafi and DNV [23][3]. These regulations are used as a basis for the propulsion system designs as well as ice impact simulations. Regulations are based on various ice-propeller interaction models and full-scale measurements conducted on various vessels. Ice impacts have been studied on several vessels in last decades, for example measurements conducted by Koskinen and Jussila on m/s Gudingen on 1991 and measurements on PRSV S.A. Agulhas II in 2011. [14] [13] [18]

Ice impacts can cause huge torque peaks in the propeller shaft, unwanted oscillation and even negative torques. All of these factors must be taken into account when designing a propulsion system for arctic waters. The propulsion system must be designed strong enough to handle the torque peaks and especially gears must be designed durable enough to withstand ice impacts. Typical problems for gears under high dynamic loads consist of scuffing, Hertzian fatigue, bending fatigue and tooth hammering – all of which can lead to gear failures. Scuffing, Hertzian fatigue and bending fatigue occur due to high oscillating loads and gear hammering occurs due to negative torque loads as the teeth of the gear detach from one another and connect again. An example of a gear failure is shown in Figure 2.2. [16]

Scuffing as a damage in bevel gears has been studied by Savolainen and Lehtovaara. There is clear indication that torque overloads cause scuffing in the gear and over-

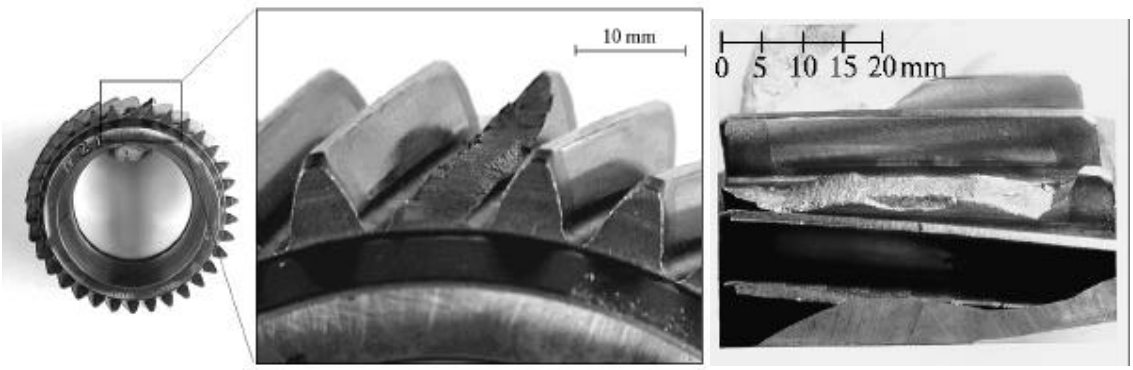

Figure 2.2. *Typical gear failure - Tooth Interior Fatigue Fracture, TIFF [16]*

loads in thrusters are often results of ice impacts. Even though scuffing in gears is not fully understood it is evident that torque peaks can cause harmful scuffing. In the study there are few remarks on how to prevent scuffing damage and under what kind of conditions scuffing usually occurs but lowering the torque peaks and overloads is one way to prevent damage to gears. [21]

2.1.1 Measured and legislation defined ice impacts

Torque loads induced by ice impacts on propulsion systems are represented as a series of sinusoidal impulses. Torque caused by ice impacts can be measured either from propeller blades or from a propeller shaft. In this paper the interest lies in the response of an ice interaction on the propeller shaft only. Because of the big inertias of the propulsion system an impact on the propeller blade is considered a sinusoidal impulse when torque is measured from the propeller shaft. Amplitude, frequency and length of the sinusoidal impulses are affected by the ice block or blocks the propeller blades are hitting, number of propeller blades and the rotational speed of the propeller shaft.

There are three different basic ice impact cases introduced in the Ice class regulations 2010 "Finnish-Swedish ice class rules 2010" [23]. These cases are listed in Table 2.1.

Table 2.1. *Ice impact cases defined by Trafi*

Torque excitation	**Ice interaction**	$\mathbf{C_q}$	$\alpha_\mathbf{i}$
Case 1	Single ice block	0.75	90
Case 2	Single ice block	1.0	135
Case 3	Two ice blocks	0.5	45

In Table 2.1, parameter Z is the number of propeller blades, C_q is the relation of

ice impact induced torque and system's nominal torque and α_i is the duration of propeller blade's interaction with ice in propeller rotation angle. In the three cases the amplitudes of ice impacts are 75 %, 100 % and 50 % of the nominal load as well as the length in angle is 90, 135 and 45 degrees, respectively. Shapes of these three ice impact cases in a propulsion system with four-bladed propeller are presented in Figure 2.3.

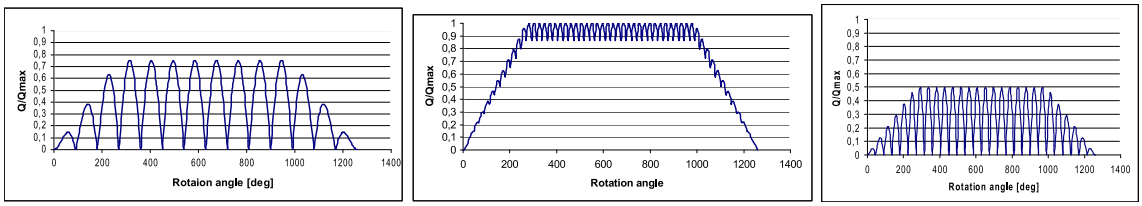

Figure 2.3. *The Shapes of the ice torque excitations on a propeller shaft [23]*

Measurements of ice impacts have been made on few different vessels in last decades and one of these measurements was conducted by Koskinen and Jussila on m/s Gudingen in 1991 [14]. The propulsion system of the Gudingen consists of propeller with 2 m diameter and four propeller blades. In the measurements, the nominal rotational speed of the propeller shaft is 379 rpm and nominal torque load is approximately 40 kNm. One part of the measurements by Koskinen and Jussila is shown in Figure 2.4. [14]

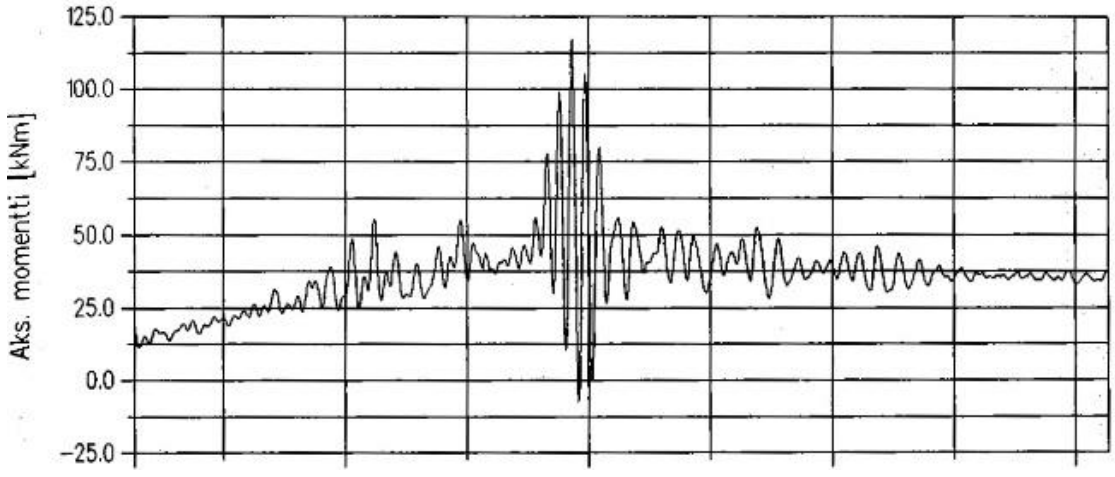

Figure 2.4. *Torque measurement on m/s Gudingen by Koskinen and Jussila. Column width in the figure is 0.5 s [14]*

Sinusoidal oscillation of the shaft can be seen in Figure 2.4, as well as the peak torque load of 117 kNm. In these measurements the maximum torque load on the propeller shaft caused by ice impact is over 2.9 times the nominal torque load of the

system and minimum value of the torque decreases below zero. Estimated duration of an individual ice impact in the measurements is 40 ms. [14]

Ikonen et al. studied ice impacts based on measurements conducted on the vessel PRSV S.A. Agulhas II [13]. Peltokorpi conducted another study of the same measurements in his Master's thesis [18]. Test system for these measurements was a variable pitch propeller with over 25 m long shaft line and 6 MW power level. During the measurements, the conditions were not ideal for ice impact studies as thickness of the ice varied between 0 and 0.7 m which is lower than the designated thickness of 2.0 m. Despite the conditions, clear ice impacts could be seen from the measurements. Two examples of ice impact responses on the propeller shaft from the measurements are presented in Figure 2.5. [13][18]

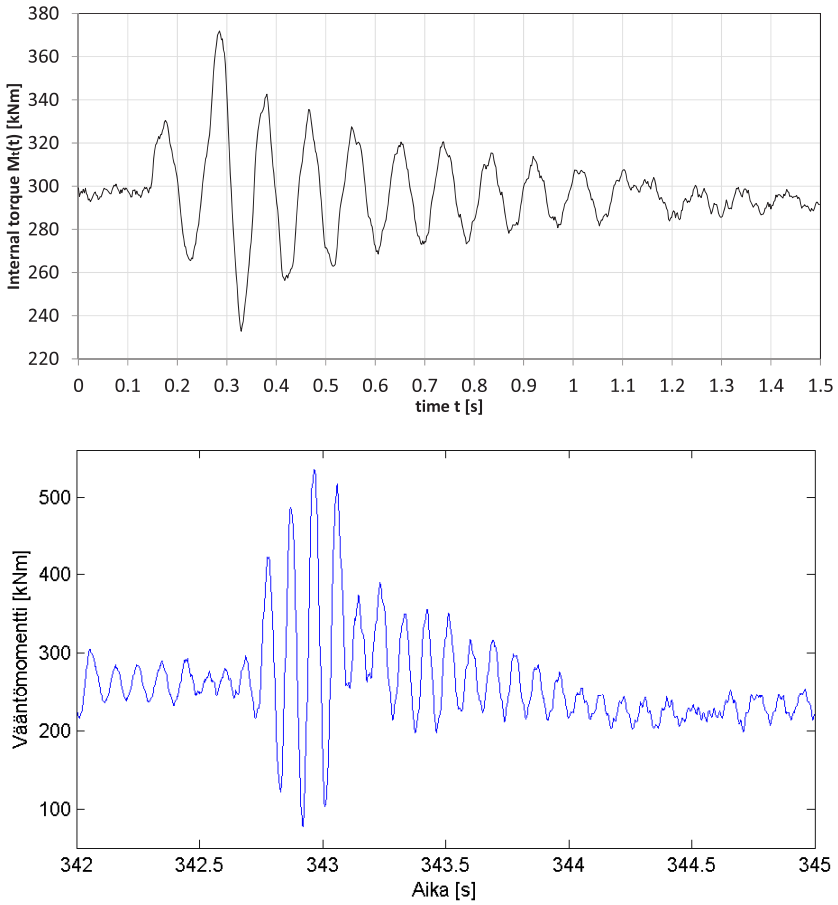

Figure 2.5. *Propeller shaft ice impact responses from the research of Ikonen [13] and the studies of Peltokorpi [18]*

Top torque response of Figure 2.5 is taken from the studies conducted by Ikonen et al. and bottom response is from the Master's thesis study by Peltokorpi. Torque in both studies is determined from the strain gauge measurements. Nominal torque in the example from the study of Ikonen et al. is 300 kNm. Torque oscillates around

the nominal value with amplitude peaking to 70 kNm. The water resistance of the rotating propeller causes the nominal torque of the propeller shaft. Torque starts to increase at 0.15 s and this can be considered as a starting time of the ice impacts. Ice impacts are estimated to last until around 0.38 s when the clear decaying of the oscillation starts. This decay is due to the damping effect of water. Individual ice impacts are estimated to last 60 - 80 ms in the study. The torque response graph from the Master's thesis of Peltokorpi shows the most sizable ice impact of the measurements. Amplitude of the most substantial ice induced propeller shaft torque oscillation is 228 kNm. Along with a nominal propeller shaft torque of slightly under 300 kNm, total torque of the propeller shaft exceeds 500 kNm. [13][18]

Simulation studies of ice impacts have been conducted by e.g. Persson in his publication Ice Impact Simulation for Propulsion Machinery [19]. The simulations by Persson have been performed with MAN corporate's GTORSI software. Propulsion system in the simulations was a 6.2 m diameter propeller with a rotational velocity range of 99 rpm. An example of the resulted simulations is presented in Figure 2.6 with torque response on the left side and velocity response on the right side. Torque peak of the propeller shaft response was around 1800 kNm with nominal loads of 590 kNm. Rotational velocity response from a similar ice impact case shows a 79 rpm average nominal rotational velocity with a drop to minimum of 39 rpm. [19]

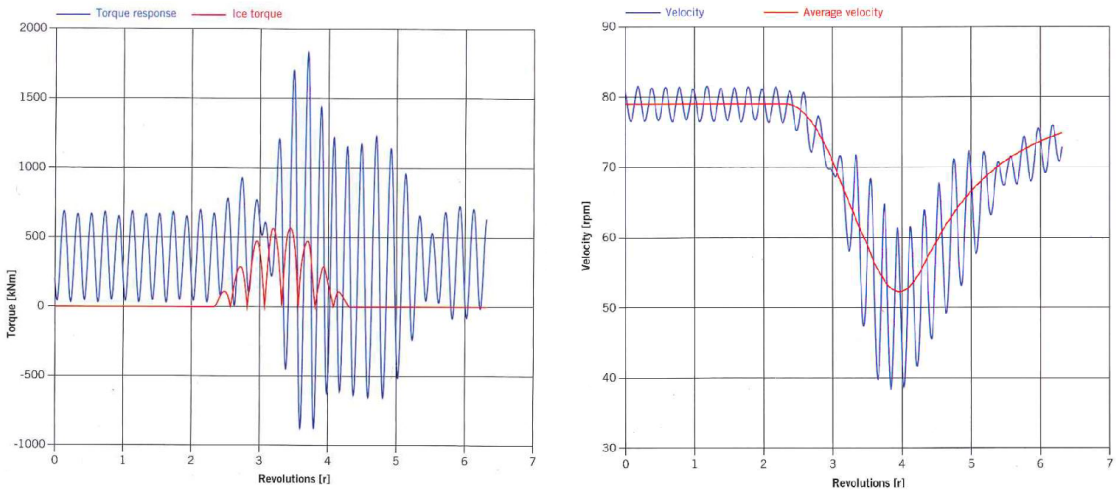

Figure 2.6. *Simulated ice impact torque and velocity responses by Persson [19]*

Ice impacts and their torque response on a propeller shaft can be simulated but problems with the simulation models come to accuracy and generalization. It is possible to generate only the most general cases of ice impacts without proper validation data.

2.1.2 Model based generation of an ice impact

Ice impact model was created to generate simulated ice impacts for the ArTEco project. Model was designed to generate all three of the ice impact cases similar to the ones presented in Ice class regulations 2010 [23]. Additionally the model was made to generate ice impacts with lower relative sinusoidal wavelength. In this model the relative length of an impact is considered 100 % when the next impact starts at the same moment as the previous impact ends. In a system with four-bladed propeller 100 % relative length means an ice impact every 90° of rotation with an impact length of 90°. With a lower relative length impacts still occur every 90° of rotation but the actual impact length is less than 90°. E.g. 45° impact length on a four-bladed propeller system would convert to relative length of 50 %.

Ice impact model has four different methods of generating impacts; modes 1 through 4. First three modes create similar impacts as in the cases 1 through 3 from the Ice class regulations 2010, respectively [23]. The fourth mode is more customizable with adjustable relative length of the sinusoidal impact. Amount of the adjustable parameters varies depending on the chosen impact mode. Main system of the ice impact model is presented in Figure 2.7 along with the mode selector. Mode selector activates the mode chosen in the parameters and causes an error if presented with an ineligible value.

Input of the ice impact model is a propeller shaft rotational velocity in rpm and output is a positive ice impact load in kNm. Propeller shaft rotational velocity in combination with number of propeller blades is converted to both cumulative rotational angle and blade hit frequency. Angle is used to create specific amount of blade hits and frequency is used to generate suitable sinusoidal waves. The ice impact induced load is to be added to an existing nominal torque load of a system.

Each different ice impact mode has a preset case. Preset cases in this report mean that neither frequency nor torque load is forced to specific value. In preset cases, the frequency of the blades hitting an ice block is calculated from the rotational velocity of the propeller shaft. Additionally maximum torque of the ice impacts is between 50 % and 100 % of the nominal load depending on the mode. Model can only generate one ice impact per simulation. Multiple ice impacts are possible to generate e.g. with the help of signal builders and pulse signals but it requires few changes inside the model itself.

First mode generates continuous sinusoidal impact with the relative length of 100 %. Ice impacts of the mode 1 are similar to the case 1 in the Ice class regulations 2010 [23]. In the preset case the maximum impact load is 75 % of the system's nominal

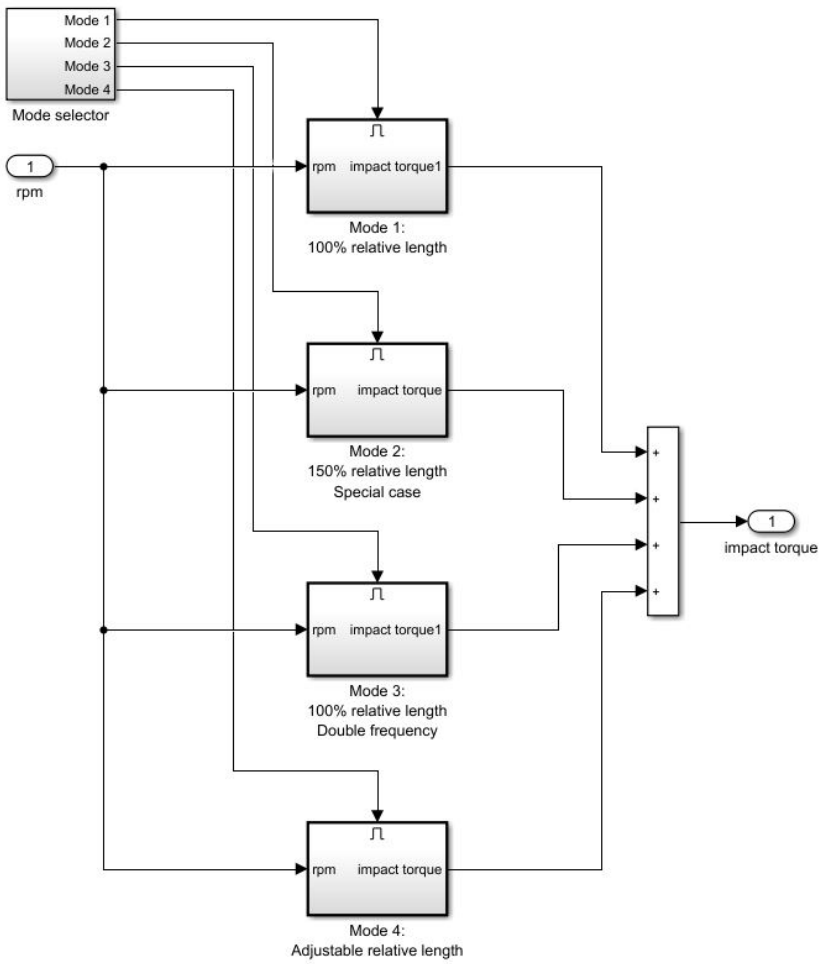

Figure 2.7. *Main system of the ice impact generator model*

load. Example simulation of the ice impact torque generated by mode 1 is presented in Figure 2.8. The nominal load is set to 38.8 kNm and thus the maximum added impact load is 29.1 kNm in the simulation example. Propeller shaft rotational velocity is a constant 320 rpm. The number of propeller blades in this simulation is set to four, which means that propeller blade hits occur every 90° and the impact length is full 90°.

In the mode 1 there is a possibility to adjust several parameters and affect the impact; number of propeller blades, nominal load torque, starting time and number of propeller blade hits to the ice block can be varied. In a preset case mode 1 memorizes the propeller blade frequency at the time the ice impacts are set to start and uses this as a constant frequency to create the sinusoidal impacts. Because of this if the rotational speed of the shaft drops in mode 1 during the ice impact, frequency of the ice impacts will not change.

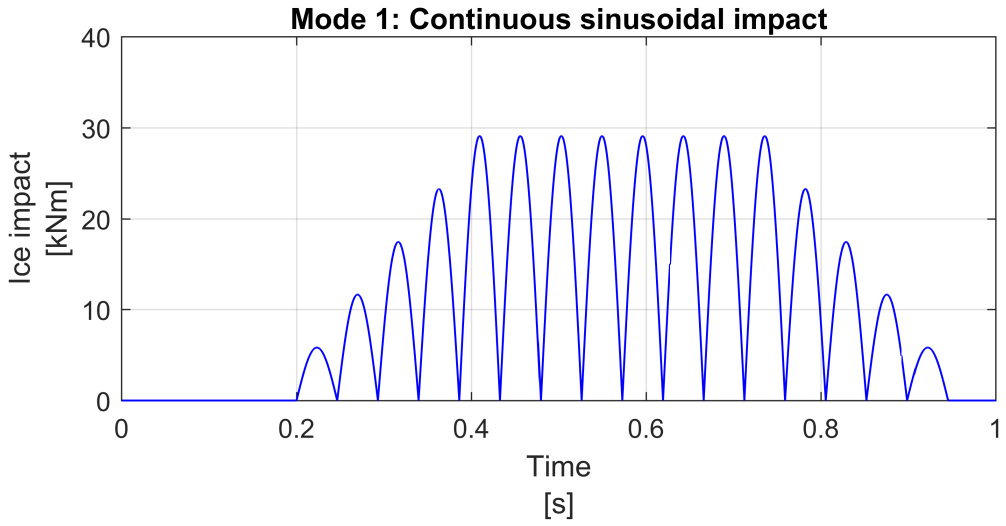

Figure 2.8. *Mode 1 - Continuous sinusoidal impact*

Mode 2 creates an ice impact that is similar to the case 2 in the Ice class regulations 2010. Mode 2 generates the ice impact differently than the other modes in the model as it sums the total impact from two sinusoidal waves. An example simulation of the mode 2 impact is presented in Figure 2.9 with identical conditions to the previous example in Figure 2.8.

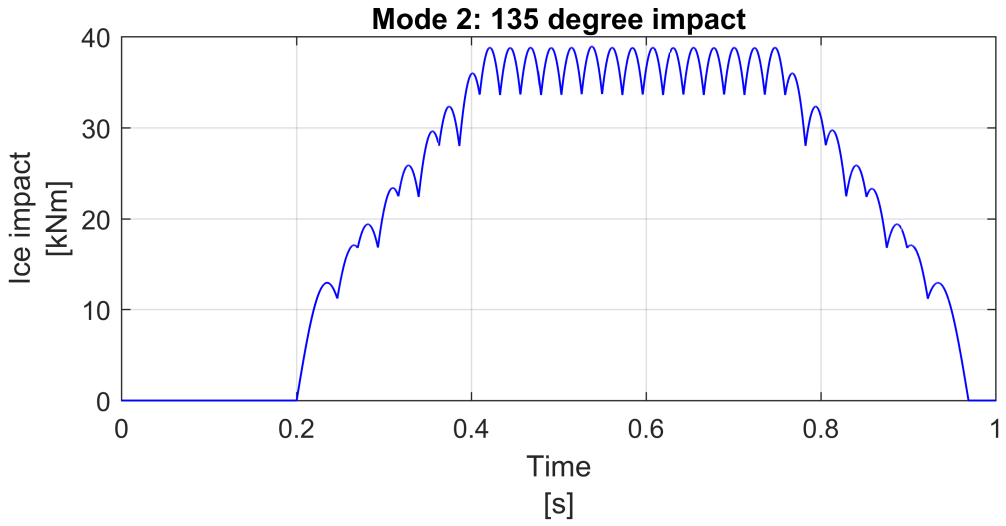

Figure 2.9. *Mode 2 - 135 degree impact*

Mode 2 is a special case in the ice impact model as many of the parameters adjustable in other modes are hard coded in this mode. Only adjustable parameters are starting time, nominal- or forced maximum load and optional forced frequency. Number of propeller blades, number of ascending and descending impacts, number of maximum load impacts and relative length of the sinusoidal wave cannot be

changed by parametrization. Number of propeller blades is set to four.

Mode 2 sums up two sinusoidal waves to create the impact. The two sinusoidal waves have 90° of difference in phase and both of the wave's individual propeller hits last for 135°. Propeller blade hits an ice block every 90°. In a preset case the maximum load of the mode 2 is 100 % of the nominal load of the propeller shaft. As it is the case with mode 1, mode 2 memorizes the frequency of the propeller shaft in the beginning of the impact and uses this constant frequency to create the sinusoidal waves for the impact if the frequency is not forced to specific value.

Mode 3 is the same as mode 1 with few exceptions. In mode 3 the frequency is doubled so that the ice impact happens twice for every propeller blade and with four blades, each impact lasts for 45°. Example simulation of an ice impact created with mode 3 is presented in Figure 2.10 with same scale and parameters as the previous simulations.

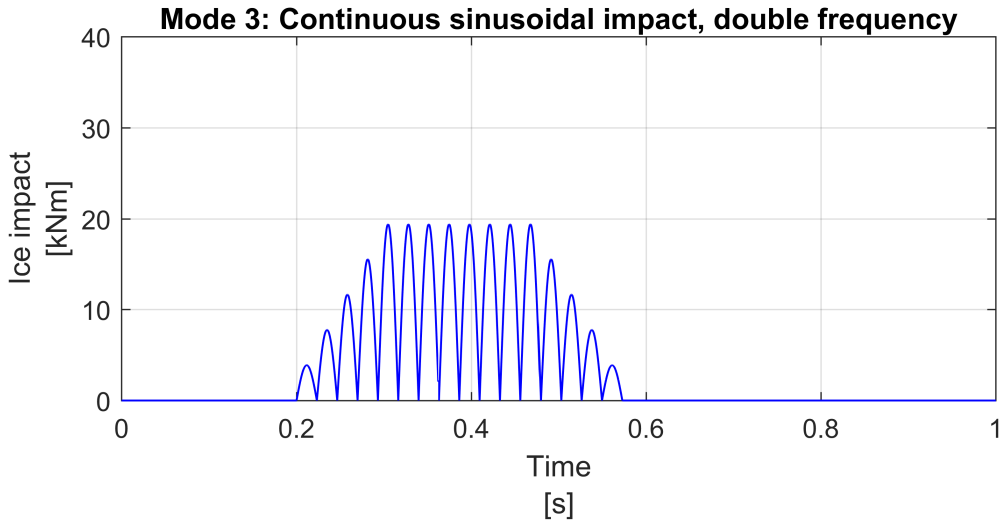

Figure 2.10. *Mode 3 - Continuous sinusoidal impact at double frequency*

Mode 3 has the same adjustable parameters as the first mode. Difference besides the frequency is the maximum impact load in a preset case. Maximum ice impact load for the mode 3 is 50 % of the nominal load, resulting in a 19.4 kNm load in the preset case. Similar to mode 1, in mode 3 maximum load and impact frequency can be set to a specific values.

Mode 4 is the most versatile and as such, it is the heaviest to simulate and most prone to errors. Mode 4 creates positive sinusoidal torque loads with varying frequency and adjustable relative sinusoidal wavelength. Due to adjustable relative length, the parameters in mode 4 must be set in carefully to avoid imperfect sinusoidal waves

and a safety mechanism is implemented to the model to avoid false information from simulations. The Simulink model of mode 4 is presented in Figure 2.11. In a preset case of mode 4, the maximum torque of an ice impact is set to 75 % of the nominal load as the case 1 of the Finnish-Swedish ice class rules 2010 is considered as the closest one to the mode 4 [23]. This is only an assumption of the maximum torque load.

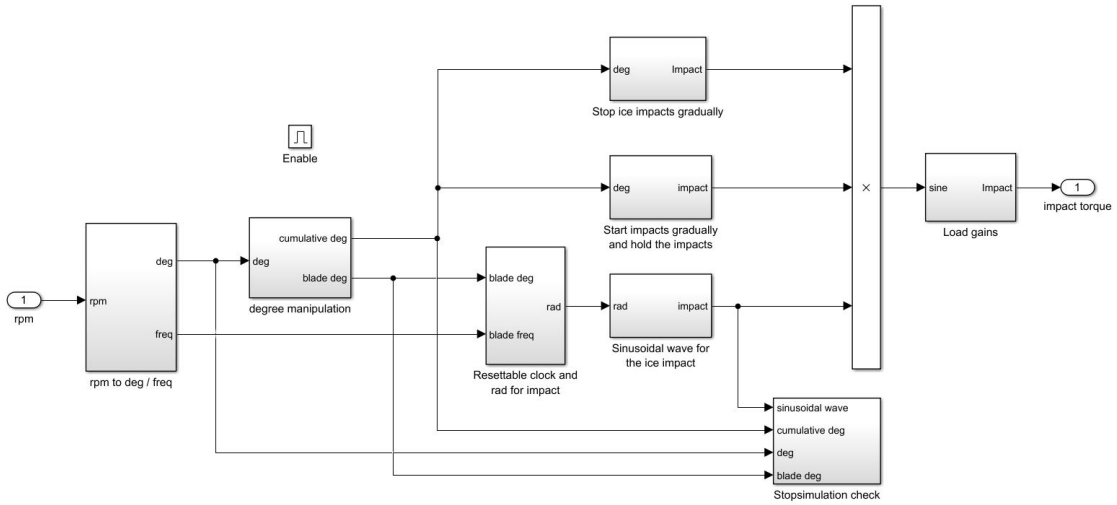

Figure 2.11. *Mode 4 - Simulink model*

Mode 4 converts the propeller shaft rotational velocity to angle and blade frequency. Most differing aspect of the mode 4 compared to the previous modes is the frequency calculation for the sinusoidal wave. Frequency is calculated individually for every sinusoidal wave and the wave is created with a ramp generated by a resettable clock that restarts every time the propeller shaft has rotated enough to pass a certain threshold. Resettable clock's threshold is the main reason why the mode 4 cannot generate ice impacts with relative length over 95 %. The other reason for this is varying rotational velocity of the propeller shaft. Relative length of the sinusoidal torque load is the most important feature in mode 4. On simulation models such as the Simulink model of the WST-14 mode 4 can handle relative lengths from over 1 % to approximately 95 % depending on the changes in the rotational velocity of the propeller shaft. The maximum relative length drops in test systems where the rotational velocity rises rapidly. Two different relative lengths are shown in a test simulation in Figure 2.12.

If a situation occurs where the propeller shaft's rotational velocity rises rapidly and the relative length is set long, the model would create an imperfect sinusoidal wave. This is due to the model not having enough time to create a full sinusoidal wave until the next impact is supposed to occur. This is prevented with a submodel that stops

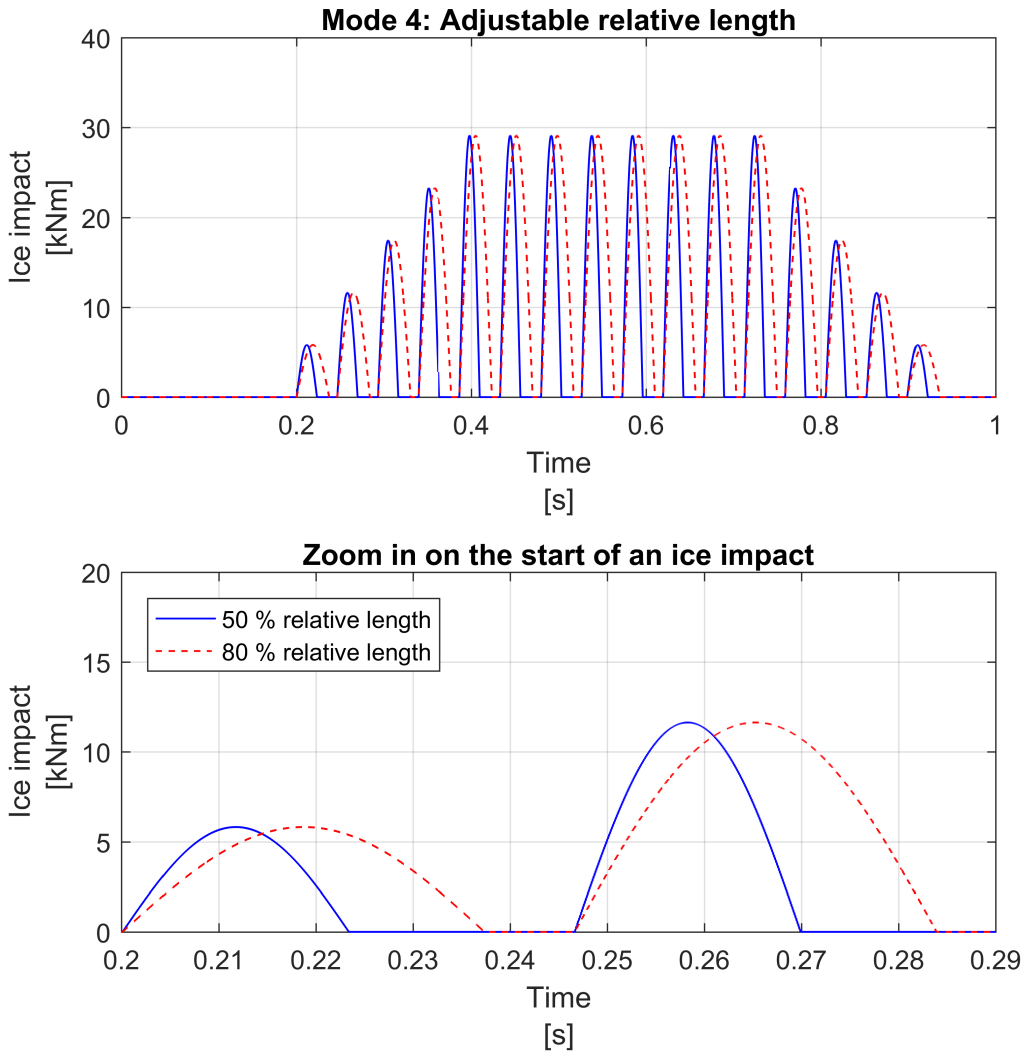

Figure 2.12. *Mode 4 - Adjustable relative length*

the simulation and results in an error if the model creates an imperfect sinusoidal wave. The imperfect sinusoidal waves are checked at the end of every ice impact series.

2.1.3 Methods of damping an ice impact

With rotational dampers there are two ways to reduce the torque peaks on a propeller shaft caused by ice impacts. First way is to tune the springs of a rotational damper to the ice impact frequency. Second way is to dampen the natural frequency resonances of the propeller shaft relating to the ice impact frequency.

Ice impacts mostly occur on a set frequency that is the propeller shaft's frequency

times the number of propeller blades. As the impacts occur on a set frequency, reducing the torque peaks with a system that is tuned directly to the ice impact frequency is possible. This method leads to bigger damper system and relatively smaller torque reduction compared to damping the natural frequencies of the propeller shaft. Damping the specific ice impact frequency is a viable way to reduce the torque peaks if there is no natural frequencies that directly correlate to ice impact frequencies.

If there is a natural frequency of a propeller shaft directly correlating to the ice impact frequency and causing resonance, damping this natural frequency can reduce torque peaks caused by an ice impact. Damping the resonance frequencies and moving the resonance peaks to more suitable frequencies is often doable with relatively smaller dampers compared to damping the actual ice impact frequency. A damping method with most effect depends on the natural frequencies and resonances of the propeller shaft as well as the whole propulsion system.

Torque peaks caused by ice impacts can also be reduced with decouplers or motor systems. Decouplers can be very effective in eliminating the effects of ice impacts, but decouplers cause relatively high losses in total efficiency of the system. If ice impacts are major concern and happen regularly a decoupler could be the most effective damping method. On the other hand if the total power of the propulsion system is high, the reduction in total efficiency can easily diminish the benefits of a decoupler.

An auxiliary motor system can be used to brake or to boost the propulsion system as an ice impact occurs or the engine of the thruster system can be controlled to reduce the torque peaks. Many studies of these methods were not found, but reducing torque peaks with these methods is possible. Damping with an auxiliary motor or with the main engine would both require very accurate and fast controllers. Detecting an ice impact and reacting to the torque oscillation by boosting or braking should all happen in a time span of mere milliseconds and thus the method is not assumed reliable way to reduce torque peaks.

2.2 Basis of rotating torsional dampers

Torsion is the twisting of a an object due to torque and in many systems such as propellers and their shafts torsion can cause severe problems such as fractures and gear failure. This is the reason why the torsion in such systems as ship's thrusters should be taken into account in the design phase. In many cases a damper is installed to a system to reduce torsion. Common dampers in high power systems

are rotational dual-mass dampers that are installed behind an engine or between an engine and transmission to reduce torsion in the engine shaft. This section of the thesis introduces the theoretical background of rotating dual-mass dampers.

It is stated in the Newton's second law of motion for a rigid body undergoing rotational motion that

$$M = I\ddot{\theta}, \tag{2.1}$$

where M is the resultant moment acting on the rigid body, θ is the angular displacement and $\ddot{\theta}$ is the angular acceleration of the system. In the equation 2.1 I is the inertia of the system. Newton's second law of motion is the basis for all the torque calculations for torsional system. [20]

Rotational dual-mass dampers are flexible couplings with two masses that have inertias of I_1 and I_2. Between the masses there is an elastic element connecting the masses with a spring constant or stiffness of K. Angular displacement of the rotating masses is denoted by θ. In a case where the flexible coupling has viscous damping or equivalent viscous damping present and either inertia I_1 or I_2 is allowed to rotate freely the flexible coupling is a rotational damper. Damping constant is denoted by C. A free body diagram of a rotating torsional damper with viscous damping and freely rotating inertia I_2 is shown in Figure 2.13.

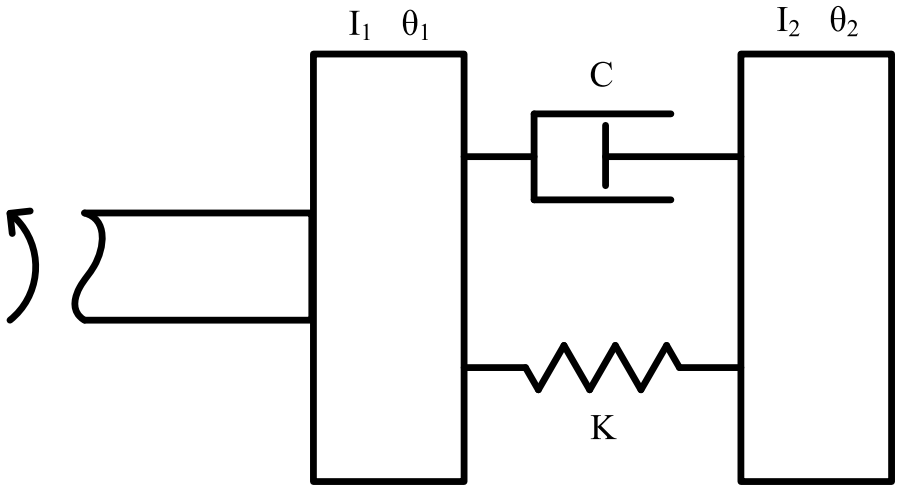

Figure 2.13. *Free body diagram of torsional mass-spring-damper*

Mathematical principle of torsional dampers can be derived using Hooke's law, Newton's law for viscous fluid and Newton's second law of motion. Hooke's law for the elastic element gives

$$T_{spring} = -K(\theta_1 - \theta_2) = -K \cdot \Delta\theta, \tag{2.2}$$

where T_{spring} torque due to the spring element and angular deflection of the two masses. The torque is negative since the direction of the restoring torque is opposite that of the deflection of the masses. Similarly to the torque produced by spring Newton's law for viscous fluid gives

$$T_{damping} = -C(\dot{\theta}_1 - \dot{\theta}_2) = -C \cdot \Delta\dot{\theta}, \tag{2.3}$$

where the damping torque $T_{damping}$ is a produce of the viscous damping constant C and the difference in angular velocities of the two masses, that is the relative angular velocity of the two elements. Damping torque also acts in opposed direction that of the difference in angular velocities.

With the equations 2.1, 2.2 and 2.3 equation of motion can be derived as

$$I\ddot{\theta} + C\dot{\theta} + K\theta = 0. \tag{2.4}$$

From the equations 2.1 and 2.4 it can be concluded that if there is a resultant moment M acting on a body, it causes angular acceleration on the inertia body that is then reduced by the spring and the damping elements. This is due to torques T_{spring} and $T_{damping}$ acting to the opposite direction compared to the inertia's torque. [20]

Spring coefficient K and damping coefficient C must both be tuned to a proper value to achieve damping in systems. If the coefficient K is not tuned to correct frequency, the damper system will not vibrate and there is no damping. Tuning of the spring coefficient K can be done with the help of the rotational speed of the system and inertia of the freely rotating mass. Aim is to reduce the torque peaks caused by ice impacts and the method used is to tune the damper to ice impact frequencies rather than natural frequencies. Tuning of the spring coefficient K can be done with an equation 2.5

$$K = (2\pi\upsilon)^2 I_2, \tag{2.5}$$

where υ is the rotational speed of the propeller shaft and I_2 the inertia of the damper wheel [22]. If the damper tuning is conducted for a thruster system and the the damping is directly done to ice impact frequencies, the rotational speed υ must be multiplied by the number of propeller blades Z.

As the spring element has been tuned, tuning of the damping coefficient C can be conducted with the help of the spring coefficient K and inertia of the wheel I_2. Tuning of the damping coefficient is done in two parts. First equation 2.6 is used to

find the critical damping coefficient of the system

$$C_c = 2\sqrt{KI_2}. \tag{2.6}$$

Critical damping C_c means that on a stepwise impulse the damping would occur most efficiently. With continuous excitation, e.g. ice impact series, another equation is required. This is due to critical damping coefficient being often far too large and dominating in continuous vibrations. Second equation 2.7 is used to find a damping factor for the system

$$\zeta = \frac{C}{C_c}. \tag{2.7}$$

Damping factors over 1 are considered overdamping and under 1 are considered underdamping [22]. Finding a sufficient damping ratio for a rotating torsional damper is complex as the aim is not to damp the natural frequency resonance peaks and damping element is related to relative rotational velocity of the damper case and wheel. Both critical damping C_c and damping ratio ζ can be used to calculate a suitable approximation for a damping coefficient C.

2.3 Review of commercial rotating torsional dampers

Many companies have their own brand and design of torsional dampers. The commercial rotational dampers are used in varied applications; most notably in agriculture, construction machinery and rail vehicles. Similar damper designs are also used e.g. in automobiles and in marine industry. Most often the dampers are either viscous dampers, mechanical spring dampers, elastic dampers or decouplers. The amount of available commercial dampers gets smaller as the system requiring torsional damping becomes bigger or more complex. Four different commercial rotating hydraulic-mechanical dampers were studied for this literature review as well as two viscous dampers and one decoupler.

Four possible locations for dampers are shown in Figure 2.14. Location 1 is behind the engine and the damper is connected to the engine shaft. This is a common place for rotating dual-mass dampers, such as viscous dampers, and a damper in this location mostly reduces the vibrations of the engine itself. Damper location 2 is in the engine shaft between engine and the thruster. This location is common for hydraulic-mechanical dampers and especially decouplers. In location 2 the vibrations originating from the thruster are reduced so that the vibrations won't harm the engine. 3rd location is in the vertical shaft or connected to UGB. Boosting or braking motor systems could be implemented to location 3. Location 4 is the thruster cone and the main focus in this thesis.

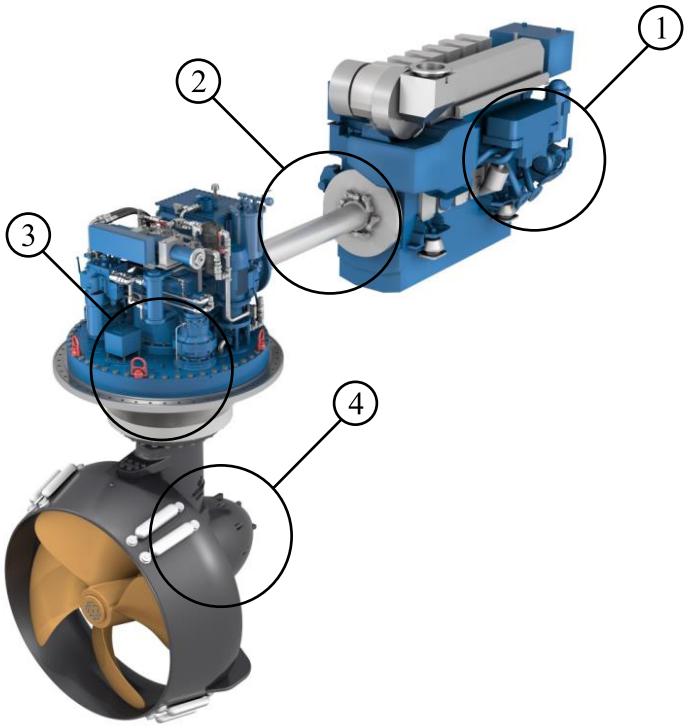

Figure 2.14. *Possible locations for dampers [27]*

2.3.1 Hydraulic-mechanical dampers

Hydraulic-mechanical dampers are rotating torsional dampers with hydraulic or fluidic elements. Hydraulic-mechanical dampers contain both primary- and secondary mass as well as a spring element connecting the two. Hydraulic part of the damper often acts as a damping or vibration isolating element.

First commercial damper to be examined is a Hydrodamp by Voith. Hydrodamp is a passive damper mainly used in agriculture, construction machinery, buses and heavy rail vehicles. The engine torques for Hydrodamp range from 1650 Nm to 3700 Nm and diameter of the damper goes up to 470 mm. It is installed between the engine and transmission. As such the hydrodamp would be too small for marine usage so modifications and scaling would be necessary. [24]

Hydrodamp uses both mechanical spring-mass system and a separate hydraulic system to produce damping. Low-stiffness springs combined with favorable mass arrangements shift the critical resonance frequencies to more suitable areas. The hydraulic part of the damper provides both vibration damping and isolation. [24]

Hydrodamp contains a floating and decoupled damping ring installed between the primary and the secondary mass, as shown in the Figure 2.15. As torsion occurs,

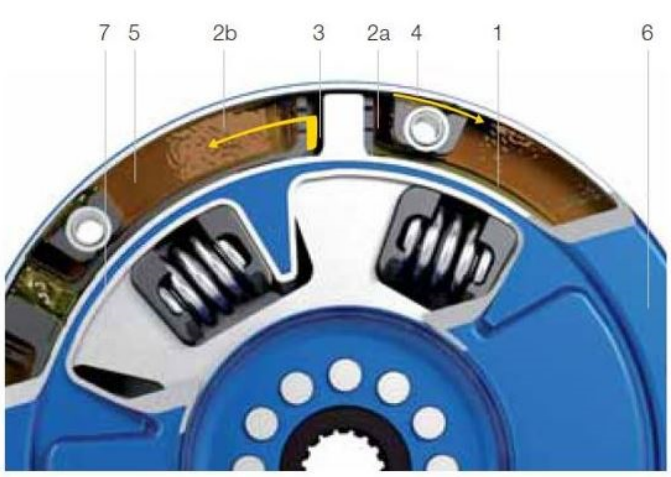

Figure 2.15. *Operating principle of Voith Hydrodamp HTSD 300 [24]*

the secondary mass of the damper starts to misalign and thus rotate the damping ring. After desired amount of backlash the rotation of the secondary mass causes pressure build-up in a chamber filled with fluid. Fluid inside the high-pressure chamber starts to flow through a damping gap to the low-pressure chamber causing torsional damping. As the fluid flows through the gaps, replacing fluid is fed to the suction chambers from inside the damper.

Hydrodamp has several segments in the decoupled damping ring forming several separate chambers. The damping effect of the Hydrodamp can be adjusted to different needs. The operating range can be regulated by adjusting the backlash of the system and the damping effect can be adjusted by damping gap geometries and viscosity of the used fluid. The damping operation should occur wear-free. [24]

Geislinger has two different torsional dampers that can be used individually or together with one another, Damper and Vdamp. The second rotating hydraulic-mechanical damper discussed is Geislinger's Damper, a tuned torsional vibration damper with mechanical springs and pressurized hydraulic oil damping.

The damping torque of the Damper is dependent on the pressure of the system. The damping torques range from 0.096 kNm/bar to 38 kNm/bar. Damper's diam-

eter ranges from 250 mm to 1800 mm and mass goes from 120 kg up to 4750 kg. Geislinger's Damper is highly scalable even up to the high torque requirements of marine vessels. Main parts of a Geislinger Damper can be seen in Figure 2.16. [4]

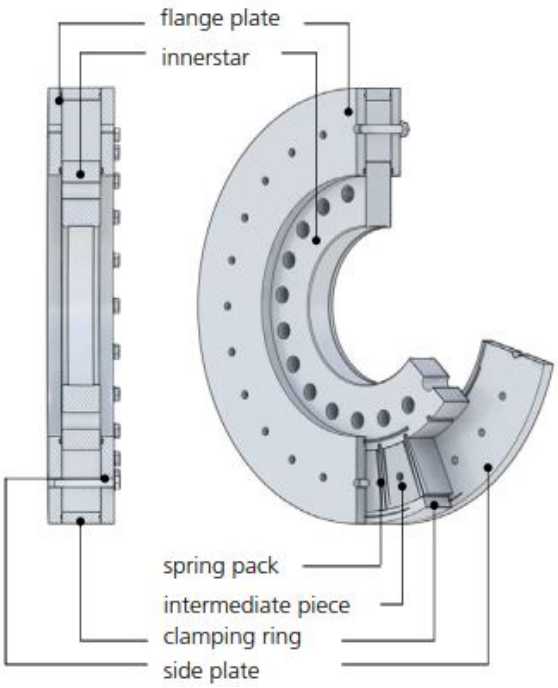

Figure 2.16. *Main parts of a Geislinger - Damper 300 [5]*

Geislinger's Damper is tuned torsional vibration damper with springs acting as a mechanical part and hydrodynamic oil damping acting as the hydraulic element. Damper is commonly installed to the free end of crankshaft or camshaft and normally used in 2- and 4-stroke diesel engines and reciprocating compressors. Also proven to function well in other applications such as camshafts, intermediate shafts and gearboxes [5].

The innerstar part of the Damper is installed to the free end of a crankshaft and the outer part and the housing act as secondary mass and large inertia. The spring packs in the Damper are important for both stiffness of the damper and the actual damping effect. The spring packs can produce any degree of stiffness regardless of the required damping. [4]

The radially arranged springs in the Damper are clamped at their outer ends and are engaged in the grooves of the innerstar. This creates two chambers around the springs as shown in Figure 2.17. As the innerstar and the outer part start to misalign due to torsion, the springs are bent. Bending of the springs causes oil to flow from higher pressure chamber to lower pressure chamber via damping gaps. The size

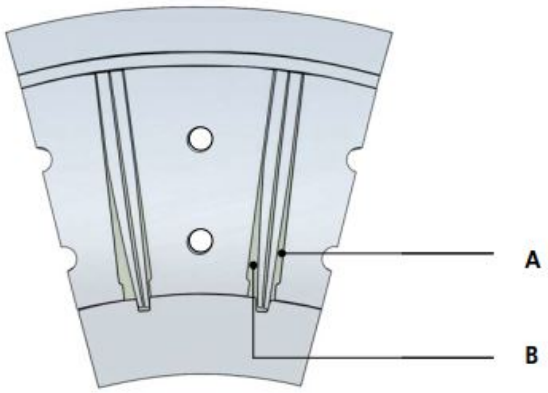

Figure 2.17. *Geislinger - Damper's spring packs [4]*

of the gaps can be modified in design phase and thus the amount of damping can be adjusted. Geislinger's Damper can be adjusted to dimensionless damping factor from 0.2 to 0.5. The damper itself is not subject to wearing. [4]

The Damper can be modified a lot depending on the needs of the system. Inertias of the system are chosen depending on the required system inertias and the stiffness is determined by the natural frequency of the system. The damping factor is calculated from the requirements of the system and required oil feed pressure is calculated from the damping torque. Because of Damper's design, it can transmit only certain damping torque without cavitation. [4]

Hasse & Wrede also has two different rotating torsional dampers available for review, Hydrolastic Damper and Torsional Visco-damper. The Hydrolastic Damper is hydraulic-mechanical torsional damper similar to the Geislinger's Damper. Hasse & Wrede as company delivers custom-built damper solutions to many of the big engine builders. The first Hasse & Wrede's damper discussed is the Hydrolastic Damper.

Hydrolastic Damper is a two-mass rotary damper, where the cone with displacing blades acts as the primary mass and the housing acts as the secondary mass. The primary mass is installed on to the free end of the crankshaft. Hydrolastic Damper is always tuned individually to the needs of the system and it is used for example in industrial engines. Main parts of the Hydrolastic Damper can be seen in the cross-section of the damper in the Figure 2.18. [8]

Mechanical elasticity of the Hydrolastic Damper is gained from arc-shaped steel springs and the hydraulic damping element is gained from the mineral oil within the displacement chambers. Damping factor of the damper is proportional to relative vibration velocity squared and thus high amplitudes are over-proportionally

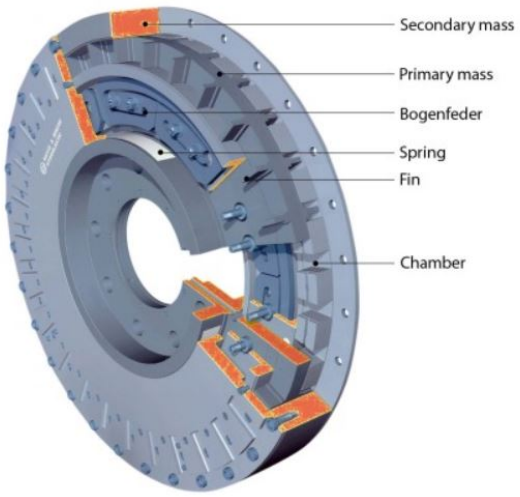

Figure 2.18. *Hasse & Wrede's Hydrolastic damper [8]*

dampened. Maximum presented engine power for the Hydrolastic Damper in the information available is 1.25 MW [9].

The Hydrolastic Damper's stiffness and damping coefficient can be tuned individually. Diameter of the commercially available dampers range from 360 mm to 1600 mm and stiffness ratings range from 0.08 MNm/rad to 16.5 MNm/rad with maximum relative vibration angle of 0.01 rad. The damping coefficient and effect must be calculated individually and the damping depends on the geometrical factor of the damper which can be altered. Damping coefficient also depends on the vibration angle occurring in the system. The dissipated damper loss rating can be calculated with the help of damping coefficient and the vibration angle. [8]

The Hydrolastic Damper's damping effect is generated by hydro-dynamic displacement. There are narrow gaps between the displacing blades of the primary and secondary mass. As primary and secondary mass misalign due to torsion, mineral oil is forced through the narrow gaps from a high-pressure chamber to low-pressure chamber. The resulting pressure gradient corresponds to hydraulic power loss. [8]

The Hydrolastic Damper has long lifetime and long service intervals. Long lifetime is expected as the damper works with hydraulic- instead of viscous damping. Damper must be cooled as it works as vibration damper constantly, not just damping the high peaks of torsion. For cooling, the damper has extra cooling slots and accurate equations for calculating the amount of heat that can be dissipated are available. [8]

Dynadamp by ZF Sachs has been especially built as a damper for irregular torsional vibrations. The damper is based on ZF Sachs' Dual-Mass Flywheel's technology and it functions as a decoupler as much as a hydraulic-mechanical damper. DynaDamp can be used for engines with torque levels up to 3.2 kNm and it is installed between the engine and the transmission [30]. Damper is commonly used in applications like construction machinery and trucks. In Figure 2.19 DynaDamp and its cross-section are presented.

Figure 2.19. *ZF Sachs' DynaDamp [30]*

DynaDamp acts as both mechanical and fluid damper. Due to the placement of the torsional damping springs and the combined speed-dependent fluid damping, rotational irregularities are reduced effectively. The spring sets in the damper contain a combination of multiple compression springs filled with fluids and this enables multi-stage characteristic curves for the damper. This leads to highly tunable dampers. [29]

As the DynaDamp is a decoupling damper, it has a primary mass that is connected to the engine and a secondary mass that is connected to drive shaft. Between the masses there are bearings that allow rotating of the masses and springs that damp the vibrations. ZF Sachs also advertises thermal stability for the damper over its entire lifetime and superior product quality via the use of large-scale series technology. DynaDamp and all of the ZF Sachs' products are developed according to the specifications of the customer. [29]

2.3.2 Viscous dampers

In this review two designs of a viscous damper are reviewed. Viscous dampers function similarly to the hydraulic-mechanical dampers in the sense that they can eliminate the torsional vibration while installed to the free end of the crankshaft.

Geislinger's Vdamp is a viscous torsional vibration damper with housing and inertia ring with highly viscous shearing fluid in-between. Diameter of the Vdamp varies from 300 mm to 4000 mm and its mass ranges from 86 kg to 27000 kg [7].

Vdamp is a viscous torsional damper used for example in 2- and 4-stroke engines, marine propulsion and power generation. The cross-section and major components of a Vdamp can be seen in Figure 2.20. [6]

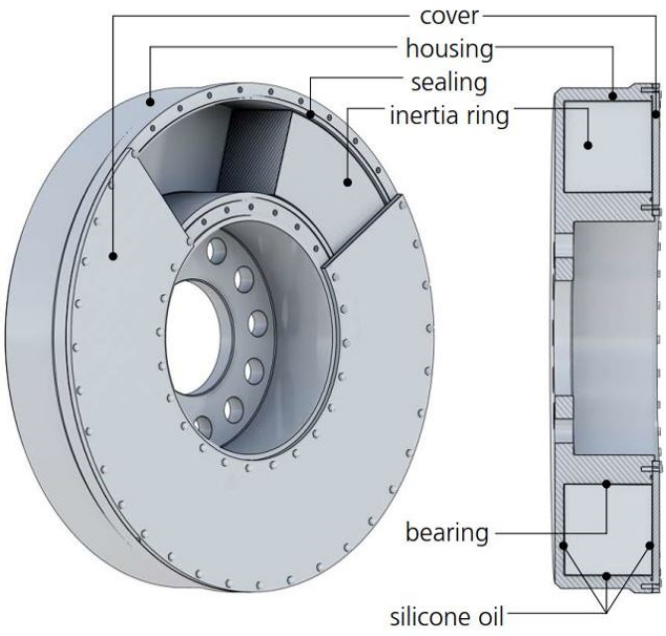

Figure 2.20. *Major components of Vdamp by Geislinger [6]*

Vdamp consists of two masses, the housing and the inertia ring guided by bearing elements. Between the two masses there is a tight shearing gap filled with highly viscous silicone oil causing damping by shearing. Shearing causes the vibrational energy to transform into heat and dissipate out through the damper's surface. Vdamp is usually installed to the free end of the crankshaft to protect e.g. propeller shaft from torsion. [7]

Silicone oil used in Vdamp shows a dependency of its stiffness and damping on both temperature and shear frequency. Together with stiffness and thermal calculations the dimensioning and vibration calculations of the Vdamp can be done.

Vdamp XT is a newer version of the basic Vdamp. Vdamp XT functions in the same way as a basic Vdamp, but it has extra reservoirs for new silicone oil. The silicone oil is subject to wearing while shearing occurs and thus needs to be changed. The extra reservoir doubles the amount of silicone oil in the Vdamp XT compared to the basic one but the change between worn out and new silicone oil must be triggered manually. There are currently no examples available on how long the viscous silicone oil will last functional under different kinds of stress. [7]

Torsional Visco-damper by Hasse & Wrede functions similarly to the Geislinger's Vdamp discussed earlier. Torsional Visco-damper is used in cars and industrial engines, even up to 2-stroke marine vessel engines. The biggest off-the-shelf Visco-damper is for 2-stroke ship engine with 80 MW power [12]. The cross-section and main parts of the damper can be seen in the Figure 2.21.

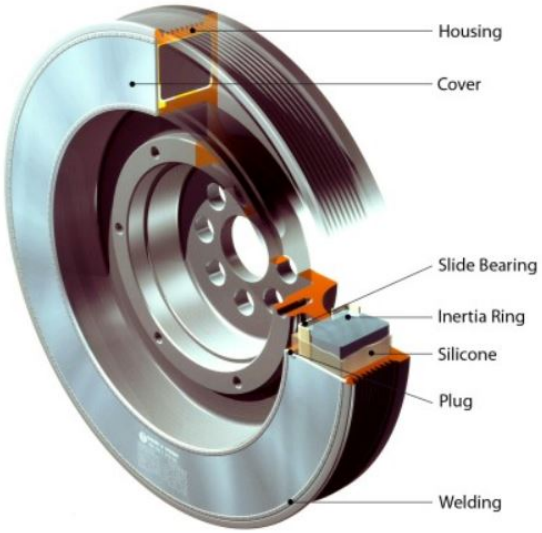

Figure 2.21. *Torsional Visco-damper by Hasse & Wrede [10]*

Torsional Visco-damper mainly consists of inertia ring and housing with slide bearing and a gap with viscous silicone oil in-between. When there are no torsional vibrations present, the primary mass of housing and secondary mass of inertia ring rotate uniformly with no damping. As the torsion vibrations start, relative motion of the masses cause shearing stress to viscous fluid damping the system. The kinetic energy of torsion vibration is thus converted into heat. The Torsional Visco-damper is installed to the free end of the crankshaft. [10][11]

2.3.3 Couplings

In this review only one coupling design is studied as a comparison point for the dampers. Couplings are widely in use in marine applications.

Vulkan Couplings' flexible couplings are used in myriad of different applications and especially in ships and boats, from small leisure boats to icebreakers. Vulkan Couplings' RATO product family is especially made to withstand very high torques and handle the torsional damping. RATO dampers can be either installed to the engine shaft to prevent engine's torsional vibration or in front of the propeller to eliminate propeller's torsional vibrations. Basic RATO DS coupling and its cross-section is shown in Figure 2.22. [26]

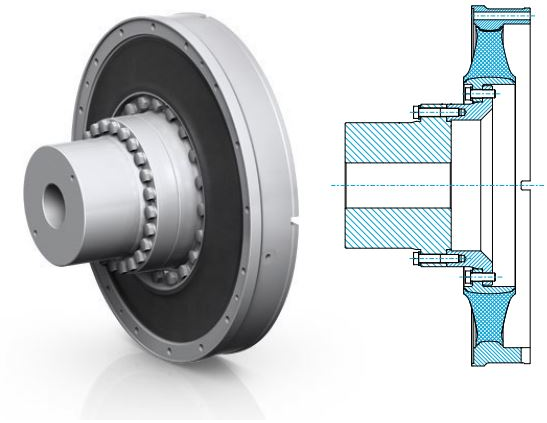

Figure 2.22. *Rato DS by Vulkan Couplings [26]*

The flexible coupling functions by decoupling the primary and secondary sides of the coupling and transmitting the torque backlash-free. The torque is transferred via fluid using the Föttinger principle.

RATO DS is specially designed for applications with high levels of torsional vibrations and its main application is ships main propulsions. RATO DS torque range is from 6.3 kNm up to 160 kNm with a maximum rotational speed of 1040 rpm.

RATO DS has several different series and configurations, but estimations for the size of the biggest 160 kNm torque coupling are 1255 mm diameter, 635 mm length and above 1 tn mass. For the smallest 6.3 kNm coupling the estimated dimensions are 645 mm diameter, 148 mm length and around 100 kg mass. Better estimation of required RATO DS dimensioning can be done with the help of Vulkan's technical brochures. [26][25]

The normal misalignments caused by foundation deflections, heat etc. can be adequately compensated for by the radial, axial and angular flexibility of the RATO DS. Dynamic safety was the prime consideration in the design of the RATO DS coupling. This is reflected in the element shape, mechanical and thermal capacity, and by using a friction-loaded bolt arrangement. The ventilation holes located in the coupling's metal parts ensure that any heat generated in the coupling is effectively removed and thereby guarantee the desired functionality of the drive system even under the toughest operating conditions. [26]

The compact dimensions of the RATO DS lead to significant weight savings and therefore increase the efficiency of the drive system and reduce operating costs. The possibility of radial removal of the element leads to easier installation and maintenance. [26]

2.3.4 Motivation for designing a novel damper

Some of the commercial dampers reviewed are suitable for marine vessels in arctic waters as such and many of the dampers could be altered to reduce vibrations in ships. It is noted that there is very little research data available. Some critical aspects of the reviewed dampers could not be found without contacting the manufacturers. Many of the dampers are also always customized to the needs of a certain systems by the manufacturer so the dampers are actually not advertised as commercial off-the-shelf products. Literature review of the commercial dampers was done as thoroughly as possible without contacting the manufacturers. Summary of the commercial dampers can be seen in the Table 2 in Appendix A.

As the commercial dampers have been reviewed it is concluded that the studied dampers would function only in locations 1 and 2 of Figure 2.14; in the engine shaft. Requirements of the project for the damper state that the damper should be located at the bottom of the thruster at the location 4. This leads to a need to design a novel rotating torsional damper. It is concluded that a damper similar to the studied hydraulic-mechanical ones would be most suitable for the project. Hydraulic-mechanical damper could be made active or semi-active and with proper design it would be nearly maintenance free. In a case of damper malfunction a hydraulic-mechanical damper would not hinder the normal operations of the thruster.

3. DESIGN AND MODELLING

Design and modelling chapter introduces a simulation model of the WST-14 propulsion system, initial dimensioning of a rotating damper as well as modelling and dimensioning of a hydraulic-mechanical damper. A validated model of the WST-14's driveline is given for the use of the thesis by the Tampere University of Technology (TUT) Laboratory of Automation and Hydraulics (AUT). Initial dimensioning for the damper is conducted so that the damper would fit into a WST-14 cone. Later an improved dimensioning and parametrization for the damper is done with the help of the Simulink model.

Model of the WST-14 propulsion system is created with Matlab's Simulink Simscape library. Damper is modelled without the Simscape library and the two are connected via sensor signals and a torque source. Solver used in the simulation model is ode15s with a maximum step size of 0.1 ms.

3.1 Predefined model of a thruster driveline

To simulate both effects of ice impact loads and dampers on a propeller shaft, a model of a thruster driveline is required. Model of a thruster driveline includes a simple PI controlled torque source that acts as a variable-frequency drive, ideal gears, flexible shafts, inertias and a propeller as well as torque loads of the thruster. The thruster model was validated with data from a test site in Tuusula Finland. The validated model is slightly different to the one used in this study as the validated model contains a generator, a gearbox and a cardan shaft instead of a propeller. For this study the generator, gearbox and the cardan shaft were replaced with an inertia of propeller submerged in water. It is assumed that the thruster model remains valid enough after these changes to give results reliable enough.

Simulink model of the thruster driveline is created with Simulink's Simscape library as well as with traditional Simulink components. Simscape enables faster modelling with ready-made physical components such as gears and flexible shafts [17]. Rotational components of Simscape are connected with a physical signal that transfers

e.g. torque and rotational velocity making these variables easier to examine. Illustrative image of the thruster driveline is shown in Figure 3.1.

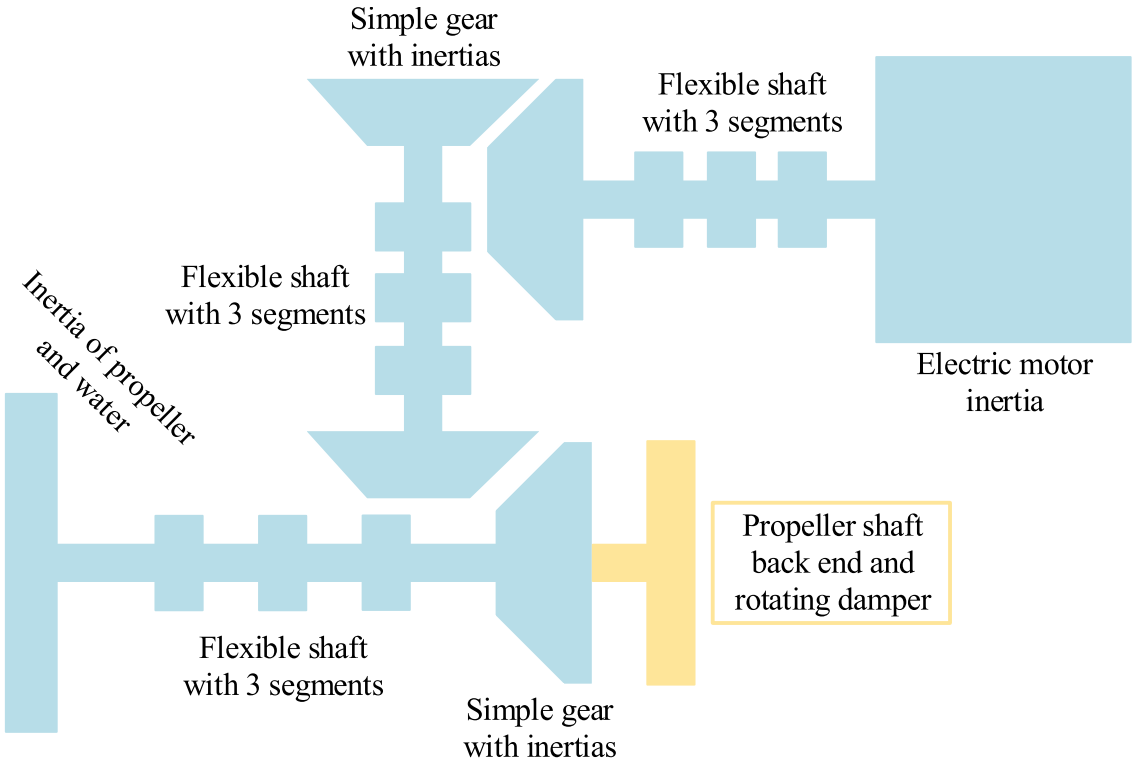

Figure 3.1. *Concept diagram of a WST-14 propulsion system model*

Electric motor of the thruster model is a tuned PI controller with an ideal torque source. Input of the PI controller is the difference between current rotational velocity of the motor and a rotational velocity reference. The rotational velocity reference contains small sinusoidal oscillation similar to the oscillation in the validation data. Output of the PI controller is a torque input to the ideal torque source. This combination provides both rotational velocity and a motor torque to the driveline. Electric motor simulates a variable-frequency drive used in arctic vessels.

Thruster model contains a total of three different segmented flexible shafts. The three shafts are an engine shaft, a vertical shaft and a propeller shaft. Flexible shafts consist of 3 segments each. More segments in flexible shafts would produce more realistic results but the simulation time would grow too long. Shafts are otherwise parametrized according to WST-14 specifics.

Two gearboxes are included in the model. UGB with a ratio of 33 to 37 is located between the engine shaft and the vertical shaft. LGB with a ratio of 14 to 39 is located in the bottom of the thruster, connecting the vertical shaft and the propeller shaft. Total ratio of the gears from the motor to the propeller shaft is approximately

0.32. Upper gearbox is only modeled with a total gearbox inertia as the engine shaft and the vertical shaft are not inspected closely for the location of the inertia to matter. Lower gearbox is modeled with both pinion and wheel inertias to provide an accurate torque response in the propeller shaft.

Propeller is modeled only as a freely rotating inertia of with a small damping element. The damping is kept minimal as it will not have effect on the damper and the realistic effect of damping is not known. Propeller inertia is lumped with the increased inertia from the surrounding water.

Load torque is fed to the propeller inertia via an ideal torque source. The load profile is a rapidly ramped up constant. In addition to the constant nominal load of 38.8 kNm the ice impact load is added to the torque load profile. In a case where the system simulations are studied without an ice impact, the ice impact generator is detached from the system.

3.2 Initial design and dimensioning of a damper

Both design and preliminary dimensioning of a rotational damper is discussed in this part. Damper consists of two inertia discs connected to the back end of a propeller shaft. Disc connected directly to the shaft is considered as the damper case. Second disc connected to the case via spring and damping elements is the damper's inertia wheel. Basic concept of a rotational damper can be seen in Figure 3.2. In the concept figure the spring element of the system is denoted as K and the damping element as C. There are two spring and damping elements to keep the rotating damper balanced in the preliminary design, but the number of these elements can be altered and the elements can be moved inside the damper.

Preliminary dimensioning of the rotational damper is done so that the system would fit in to an existing WST-14 cone. Approximate dimensions inside the thruster cone for a round damper are radius of 300 mm and length of 200 mm. Radius of the shaft connecting damper case to the propeller shaft is assumed 100 mm. If the material used for the damper is steel, the approximate density can be set to 8000 kg/m^3 for the calculations. Now the inertias of the damper case and wheel can be calculated with an inertia equation of a hollow cylinder as follows

$$I = \frac{\pi}{32}\rho L(D_o^4 - D_i^4). \tag{3.1}$$

In the equation 3.1 ρ is density of the material, L is length of the hollow cylinder, D_o is the outer diameter of the cylinder and D_i is the inner diameter. Inner diameter is

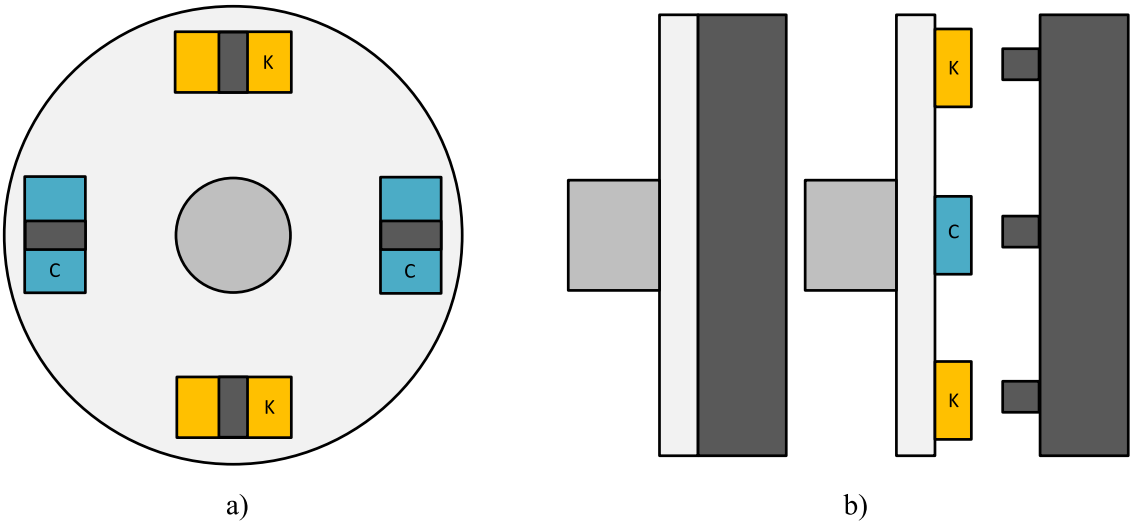

Figure 3.2. *Basic concept of a rotational damper*

neglected as the inertia of damper wheel is calculated for the wheel is considered a solid wheel. Effective damping inertia of a rotational damper is the damper wheel's inertia, so it is first decided that most of the available length, 150 mm, is for the damper wheel. Rest of the available length of 50 mm is for the damper case. With these parameters inertia of the damper case I_1 is 5 kgm^2 and inertia of damper wheel I_2 is 15 kgm^2. Masses of the damper case and wheel can be calculated with the density and dimensions of the system. In this case the damper case would weigh 100 kg and wheel would weigh 340 kg. These values are approximations for design as the changes in inertia and weight caused by spring and damping elements are not taken into account. Considering the inertias of the propulsion system, e.g. the inertia of propeller in water which is approximated at 430 kgm^2, it can be assumed that the initial dimensions must be altered in order to design an effective damper.

In the initial design the rotational speed of the propeller shaft is set to 320 rpm which is approximation of the full speed of the thruster. Four propeller blades are used as the design is conducted for the WST-14. For initial design a calculated spring coefficient K is 269.5 kNm/s with the equation 2.5. Calculated value for K is rather large if it is compared to typical similar size springs, but it is expected as the combined frequency of the propeller blades is over 21 Hz.

Damping factor for this damper concept must be kept low in order to achieve damping, as most of the torque reduction is caused by the spring element rather than the damping element. Damping ratio ζ of 2 % is used as an initial approximation. With the equations 2.6 and 2.7 by Thomson [22] an initial design value of 80.4 Nms/rad can be calculated for the damping coefficient C.

3.3 Hydraulic-mechanical damper design

Basic concept of the hydraulic-mechanical damper is the same as in spring-mass-damper system. In an ideal lateral spring-mass-damper system the spring is considered to be connected to a rigid base from the one end and to the damper from the other end. In a torsional spring-mass-damper system the spring is located between the damper case and wheel, transferring torque between the two, but the system is considered ideal similar to the lateral system. Spring coefficient K is considered constant.

Hydraulic spring system was to be designed in order to create realizable system. It was decided that the relative angle between the damper case and wheel is changed to lateral displacement with mechanical design. Two major design ideas were considered for a hydraulic spring. First design idea was to create a hydraulic spring element with several hydraulic nitrogen accumulators. This design was considered to be too hard to manufacture in a proper size and too unpredictable due to heavy compressibility of the nitrogen under strong forces. Second and more promising design was a pressurized hydraulic cylinder with piston resting in the middle position. Concept of the second hydraulic spring design can be seen in Figure 3.3.

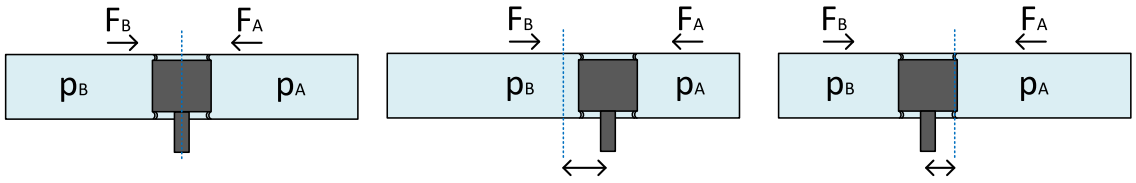

Figure 3.3. *Concept of a hydraulic spring element*

In Figure 3.3 p_A and p_B are cylinder chamber pressures and F_A and F_B are the forces generated by said pressures. Chamber pressures of the hydraulic spring can be calculated as follows

$$p = \frac{xA_{piston}B_{oil}}{V_{init}} + p_{init}, \tag{3.2}$$

where the x is displacement of the piston, A_{piston} piston area, B_{oil} bulk modulus of oil, V_{init} the initial volume of the chamber and p_{init} the initial pressure in the chamber. In a real scenario the bulk modulus of oil would be changed to total bulk modulus of the cylinder which would also change in relation to temperature and pressure, but with high enough pressures the change is considered negligible for simulations. The forces generated by the chamber pressures follow the equation 3.3

$$p = \frac{F}{A}. \tag{3.3}$$

In the equation 3.3 p can be considered the chamber pressure, A the piston area and F the generated force. In Figure 3.3 the left image is a scenario where there is no relative angle between the damper case and wheel and thus no displacement x. Volumes of the chambers are identical to one another so this leads to equal pressures p_A and p_B as well as equal forces F_A and F_B. As the forces are directly opposite, they cancel each other out and there is no total spring force generated by the hydraulic spring.

In the middle and right hand side cases of Figure 3.3 there is relative angular displacement between a damper case and a wheel. This leads to displacement of the piston from the middle of the cylinder chamber. In the middle case the displacement is towards the A chamber and this causes pressure p_A to increase in the chamber as it is stated in the equation 3.2. Similarly the chamber pressure p_B decreases. This leads to force F_A growing greater than force F_B. Total force generated by the hydraulic spring can be calculated as $F_{tot} = F_A - F_B$ and the total force is now to the same direction as F_A. In the right hand side case the displacement is to opposite direction and the displacement is smaller compared to middle case. In the right hand side case the force generated is now to the same direction as F_B but as the displacement is smaller, the total force is also smaller.

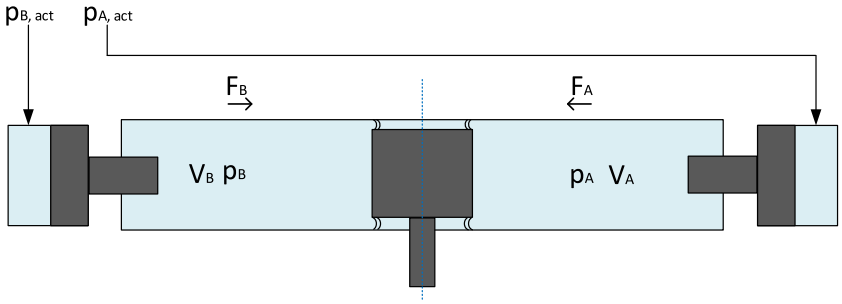

Figure 3.4. *Concept of a semi-active hydraulic spring*

For variable damping scenarios either an active or a semi-active hydraulic spring is required as the damper must be tuned to required frequency. In the previously described design of a hydraulic spring, spring generated forces and thus the spring constant K can be altered by changing the initial volumes of the cylinder chambers. In a passive hydraulic spring the chamber volume is calculated to match one specific spring constant and this is how the spring is tuned. Passive hydraulic spring can be made active with additional secondary pistons that reduce or increase the chamber volumes. These pistons can be operated with secondary chamber pressures $p_{A,\ act}$ and $p_{B,\ act}$. Secondary chamber pressures can be either actively controlled from above the thruster or semi-actively controlled with a hydraulic pump that follows the rotational speed of the propeller shaft. Concept of an active or a semi-active

hydraulic damper can be seen in Figure 3.4.

Similar to the hydraulic spring design also a hydraulic damping system was to be designed for a realizable damper. Forces generated by a damping element C are related to the relative angular velocities of damper case and wheel. Torques and angular velocities of a hydraulic damping element are again translated to lateral forces and velocities with mechanical design of the damper. Concept of a hydraulic damping element can be seen in Figure 3.5.

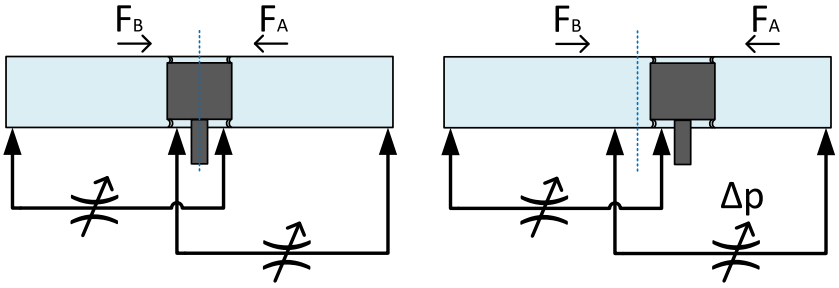

Figure 3.5. *Concept of a hydraulic damping element*

Hydraulic damping element consists of a cylinder chamber, piston, two valves and pipes connecting the hydraulic components as it is seen in Figure 3.5. Forces F_A and F_B are generated with the equation 3.3. Compared to the hydraulic spring, the initial pressures of the chambers are set significantly lower. As it can be observed from the left hand side figure, if the piston is not moving there is no pressure difference Δp and forces F_A and F_B are equal. As the piston starts moving like it is shown in right hand side figure, a pressure difference Δp is generated by the fluid flowing through an orifice. Pressure difference follows the equation 3.4 for both cylinder chambers

$$\begin{aligned} \dot{p} &= \frac{B_{eff,A}}{V_{init,A} + A_A x}(Q_A - K_L(p_A - p_B) - A_A \dot{x}) \\ \dot{p} &= \frac{B_{eff,B}}{V_{init,B} + A_B(x_{max} - x)}(Q_B - K_L(p_A - p_B) - A_B \dot{x}), \end{aligned} \tag{3.4}$$

where B_{eff} is the effective bulk modulus of a chamber and Q is the fluid flow rate. Also in this equation K_L is a laminar leakage coefficient, $\dot{x}$ is the velocity of a piston and x_{max} is the maximum cylinder length [15]. The fluid flow of the cylinder chamber Q over the valve orifice follows equation 3.5 as follows

$$Q = \mu A \sqrt{\frac{2(p_1 - p_2)}{\rho}}. \tag{3.5}$$

In this equation μ is the flow coefficient of the orifice and A is the area of the orifice. It can be observed from the equations 3.4 and 3.5 that the fluid flow through an

orifice depends on the area of the orifice and thus the pressure difference Δp can be set to desired value by changing the orifice area. This is done either by selecting a suitable valve or by using a controllable valve. Controllable valves can be utilized in a case where an active hydraulic damping element is required.

3.4 Modelling a rotating torsional damper

Matlab Simulink model of a rotating damper is attached to the model of the WST-14 propulsion system model via Simscape's physical signals. Additional propeller shaft back end that is relatively short compared to the propeller shaft is added to the system to include a connecting shaft to the damper. Connection of the damper to the propulsion system can be seen from Figure 3.6.

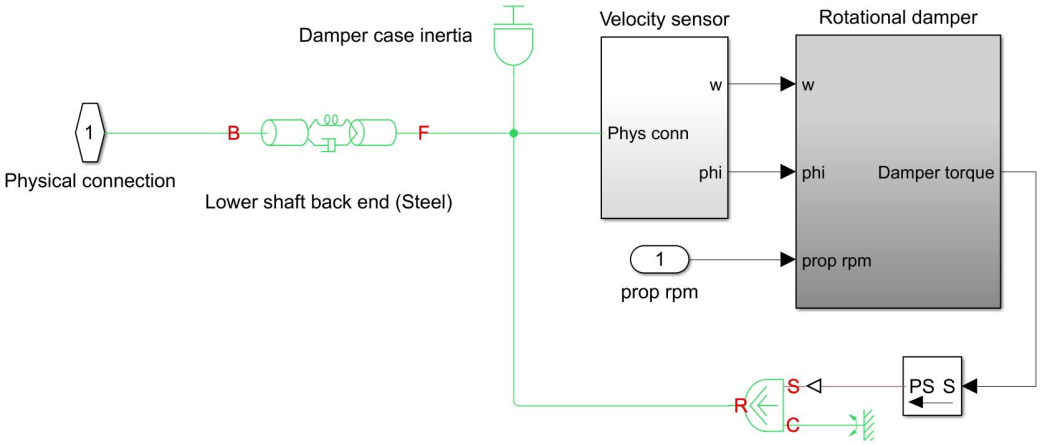

Figure 3.6. *Damper connection to the propeller shaft*

Inertia of the rotational damper's case is included in the model as a physical Simscape component. After the case inertia the physical signal is transformed to pure Simulink signals that represent rotational velocity and angle. For active or semi-active dampers, the propeller shaft rotational speed is taken from the thruster model and input to the rotational damper model. Output of the damper model is a relative torque caused by the relative rotational movement between the damper case inertia and the damper wheel inertia inside the model. As the WST-14 propulsion system is now modeled, next step is to perform linear analysis and generate a bode diagram of the system with Simulink's linear analysis toolbox.

Linear analysis of the system is done with constant load torque of 38.8 kNm and constant rotational velocity of 320 rpm in the propeller shaft. From the bode diagram of Figure 3.7 it can be observed that the first natural frequency of the propeller shaft is 30.1 Hz and marked with a blue line, the propeller blade frequency at 21.4 Hz.

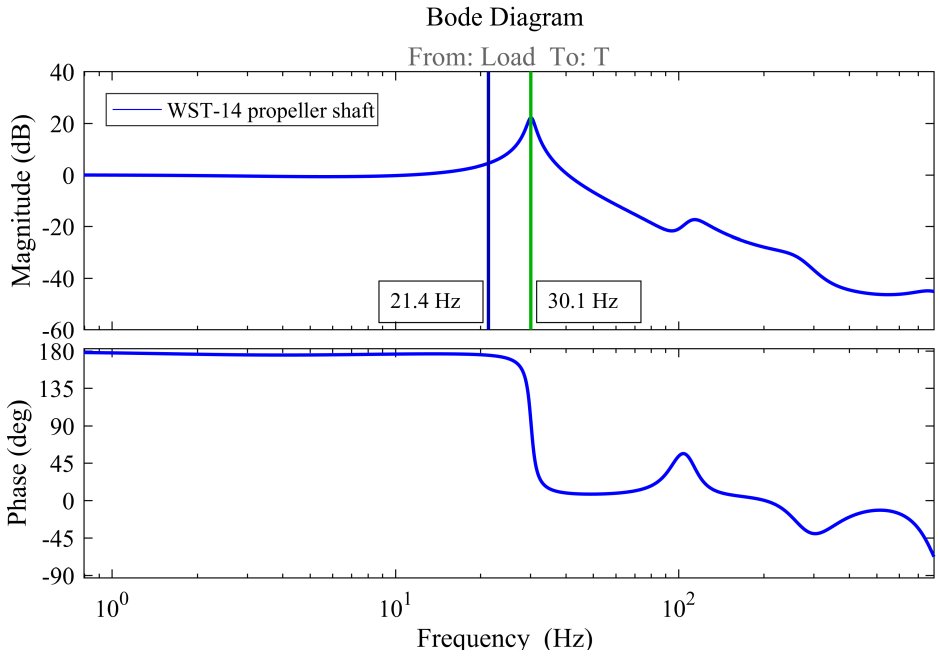

Figure 3.7. *Bode diagram of the simulation model of WST-14 propeller shaft*

This means that damping the first natural frequency of the propeller shaft will not reduce ice impact induced torque peaks. The bode diagram is considered to be a good approximation of the real system as the propulsion system is validated and similar values were found by VTT in their simulations during the project.

3.4.1 Modelling a passive ideal damper

First step in modelling a damper is a passive ideal damper. Passive damper is mathematically ideal as the model follows the equation 2.4 with constant coefficients K and C as well as damper inertias initially calculated in the design phase. A Simulink model of a passive ideal damper is shown in Figure 3.8. Passive ideal damper model is inside the ”Rotational damper” in Figure 3.6. Inputs for the model are rotational angle θ_2 and rotational velocity of the damper case $\dot{\theta}_2$. These are then converted to relative angle and relative rotational velocity $\Delta\theta$ and $\Delta\dot{\theta}$, respectively. Output of the passive damper model is the generated torque.

As the passive ideal damper is modelled and initially dimensioned, as well as the WST-14 propulsion system, more linear analysis can be performed. It is assumed that the initially dimensioned damper will not have much impact on damping the propeller shaft. With the help of both the bode diagram and simulation iterations the passive ideal damper can be improved, but this leads to damper being too big to fit in a WST-14 cone.

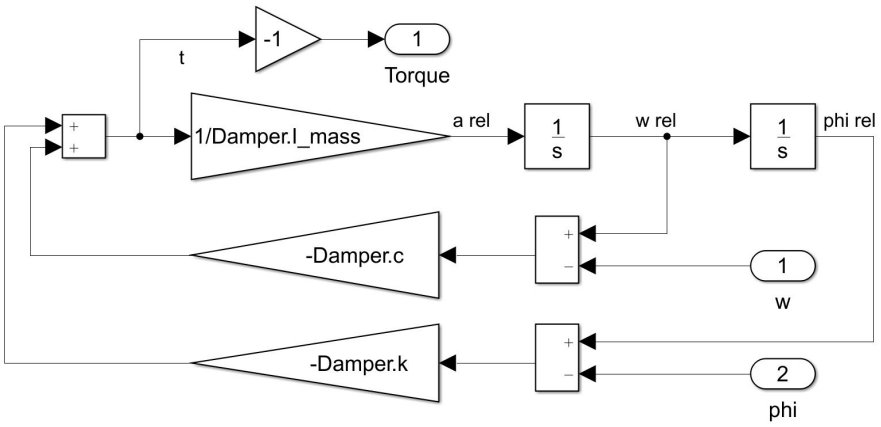

Figure 3.8. *Simulink model of a passive damper*

3.4.2 Modelling a hydraulic-mechanical damper

Passive ideal damper is now simulated and dimensioned. Next step is to create a Simulink model of a hydraulic-mechanical damper. Simulation model of the hydraulic-mechanical damper is created by first changing the relative rotational angle and -velocity to linear displacement and velocity as suggested in the concept of a hydraulic-mechanical damper. Next step is to replace the ideal spring element K to a model of a hydraulic spring and the ideal damping element C to a model of a hydraulic damping element. Simulink model of a hydraulic-mechanical damper can be seen in Figure 3.9

Simulation model of a hydraulic spring element has four main submodels. Submodels are two cylinder chambers, friction model and a semi-active control of the spring coefficient. Inputs to the hydraulic spring element are displacement x, velocity v and rotational speed of the propeller shaft rpm. Output is total torque generated by the hydraulic spring. Simple Simulink model of the hydraulic spring element can be seen in Figure 3.10.

Two cylinder chambers are modeled after simple hydraulic accumulators as there is no direct input of fluid flow to the chambers. Hydraulic spring's cylinder chambers are modeled after a pressure equation 3.6 of fluid's compressibility

$$\Delta p = -B\frac{\Delta V}{V}, \tag{3.6}$$

where Δp is the change in pressure, B is the bulk modulus of the compressing oil and V is the volume of a chamber [15]. Equation 3.6 is true only if the ΔV is much smaller than the volume V; which holds true in this case. Chamber model does take

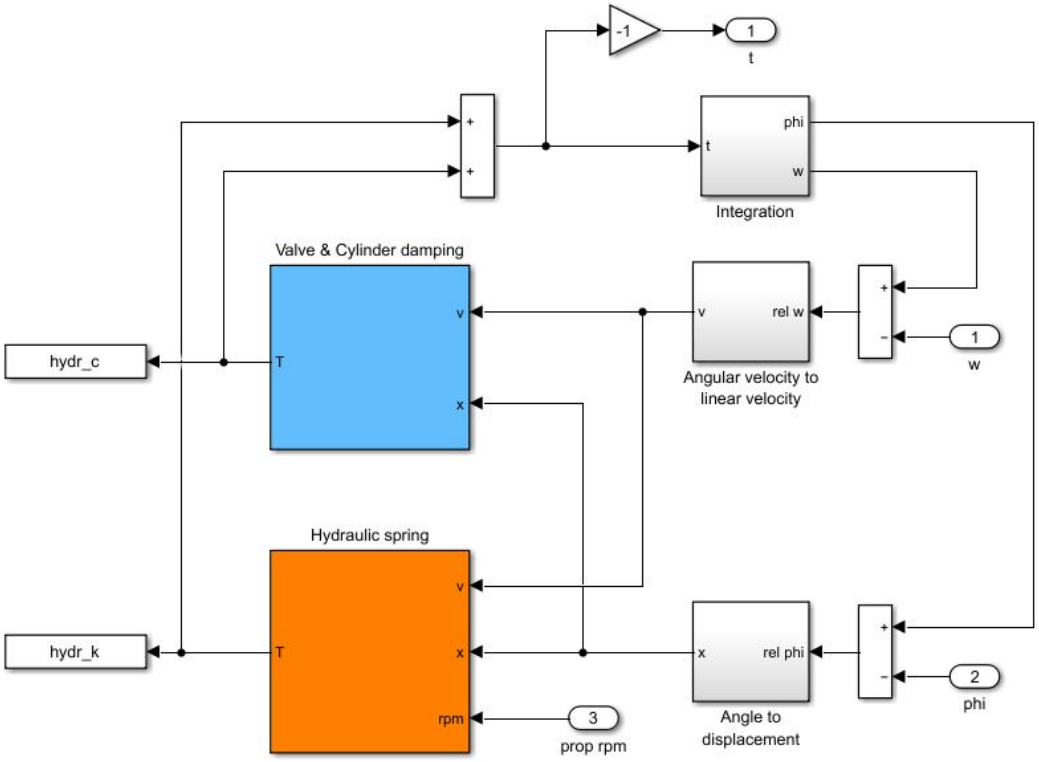

Figure 3.9. *Simulink model of a hydraulic-mechanical damper*

into account the initial pressure of the chamber but the change in bulk modulus is not modeled. With high pressures the change of B is considered negligible.

As it can be seen from Figure 3.10, model of the hydraulic spring contains a friction model. Friction model is a ”tanh” model that has static friction force and Coulombian friction force with viscous friction and a hyperbolic tangent function lumped together following equation 3.7

$$F_\mu(\dot{x}, p_A, p_B) = tanh(K\dot{x}) \times (F_C + (F_S + F_C)e^{-(\dot{x}/v_S)^2}) + b\dot{x}. \tag{3.7}$$

In the friction equation 3.7 F_μ is the total friction force, K is a parameter that determines speed of the change of the friction near zero velocity. Velocity is denoted as $\dot{x}$, v_S is the velocity of minimum friction force and b is a viscous friction coefficient. Finally F_S and F_C are static friction and Coulombian friction forces, respectively. Properly parametrized friction model sums up all the friction forces of a cylinder system into one total friction force. This force is then summed up to forces generated by hydraulic spring and the sum is lastly translated from linear force to rotational torque. Same friction model is used in both hydraulic spring and hydraulic damping model with different parameters.

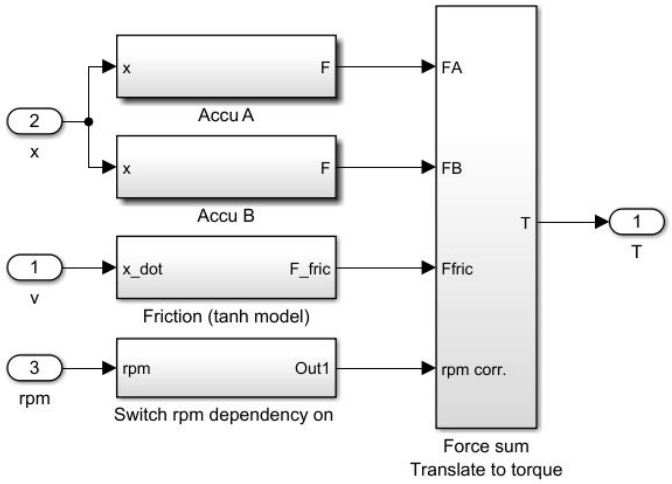

Figure 3.10. *Simulink model of damper's hydraulic spring*

Simulation model of the damping element consists of three submodels as seen in Figure 3.11. Valve open signal model acts as an active component that determines the magnitude of damping. Valve model acts as controllable valve with pressures p_A and p_B and opening signal as inputs and fluid flows Q_A and Q_B as outputs. Input pressures of the valve model are considered the pressures before and after the valve orifice, which translate directly to cylinder's chamber pressures p_A and p_B. Inputs of the cylinder model are piston displacement x and piston velocity v similar to the hydraulic spring model as well as the fluid flows of the chambers Q_A and Q_B. Outputs of the cylinder model are chamber pressures p_A and p_B as well as the total force generated by the damping element which is converted to torque.

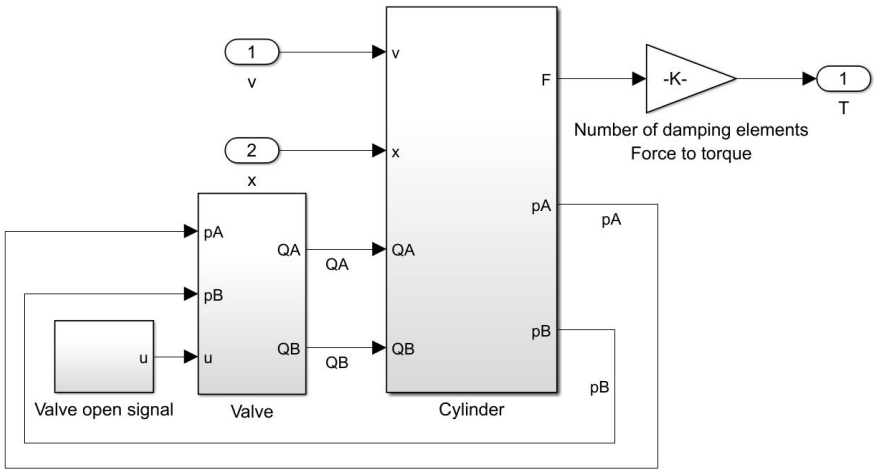

Figure 3.11. *Simulation model of a hydraulic damping element*

Cylinder model consists of two cylinder chamber submodels and the friction sub-

model. Forces generated by said submodels are summed up and this results in generated total damping force. Submodels of cylinder chambers follow the equation 3.4. Valve model follows the equation 3.5 of fluid flow through an orifice with the opening signal and valve opening dynamics as additions to the system. Simulink models of cylinder, valve and friction are all created according to Linjama's lecture materials of the course Modelling of Fluid Power Components of 2006 [15].

Both hydraulic spring and hydraulic damping element must be tuned correctly to reduce torque peaks caused by ice impacts. Tunable parameters for the hydraulic spring are initial chamber pressures, piston area, chamber volume, number of hydraulic spring elements in the damper and the location of the spring elements. Initial chamber pressures must be set high enough to allow pressures to drop in the chambers without cavitating but also low enough that the pressure peaks will not exceed safe physical limitations. Both piston area and chamber volume affect the resulting force directly as the force is generated by area and pressure difference. Pressure difference caused by moving piston is directly affected by the chamber volume. Number of the hydraulic spring elements H changes the force required to be generated by $1/H$ and number of the hydraulic spring elements can be altered freely. Location of the spring elements is the length from the middle of the damper to the hydraulic spring element. This length is used as a lever arm to convert the force generated by the hydraulic spring to torque.

Spring element will initially be tuned to the nominal rotational speed of the propeller shaft. With a completely passive system, if the thruster is not driven with the nominal speed, the damper will not reduce the torque peaks caused by ice impacts. This is why an active or a semi-active system is required. In the hydraulic-mechanical damper model the rotational velocity dependency is created by multiplying the generated spring-force with a dependency-factor γ. Factor γ is calculated with the equation 3.8

$$\gamma = \upsilon^2/\upsilon_{nom}^2, \tag{3.8}$$

where the υ is the current rotational speed of the propeller shaft and υ_{nom} is the nominal rotational speed of the shaft. This rotational speed dependency leads to spring coefficient K_{hydr} to always be tuned to correct ice impact frequency. In reality the semi-active tuning would be done with auxiliary cylinders that alter the cylinder chamber volumes, but a simplified system will be used in the simulations.

Hydraulic damping element must also be tuned correctly. All of the same parameters can be altered as in the hydraulic spring element with additional parameters coming from the valve. Tunable parameters related to the valve are valve size and valve opening. Valve size determines the maximum fluid flow between the cylinder

chambers and thus the minimum damping force generated by the damping element. Valve opening u determines current and maximum damping force by restricting the fluid flow between the cylinder chambers. Tuning of both hydraulic spring element K_{hydr} and hydraulic damping element C_{hydr} is done with the help of the simulation models of the elements and the ideal values of K and C.

3.5 Hydraulic-mechanical damper dimensioning

It was assumed that the initial parameters of the passive ideal damper would not be sufficient to have big enough effect to reduce the torque peaks. This is first proven with a bode diagram and improvements on the parameters are done accordingly. In the Figure 3.12 there is a magnitude plot of a bode diagram of the WST-14 propeller shaft without a damper, with initially dimensioned damper and bigger improved damper. Figure is zoomed to the crucial frequency of the propeller blades. The green line in the figure represents the propeller blade frequency and also the tuning frequency of the dampers. The red line represents an estimated maximum drop in the rotational velocity of the propeller shaft that is 10 %.

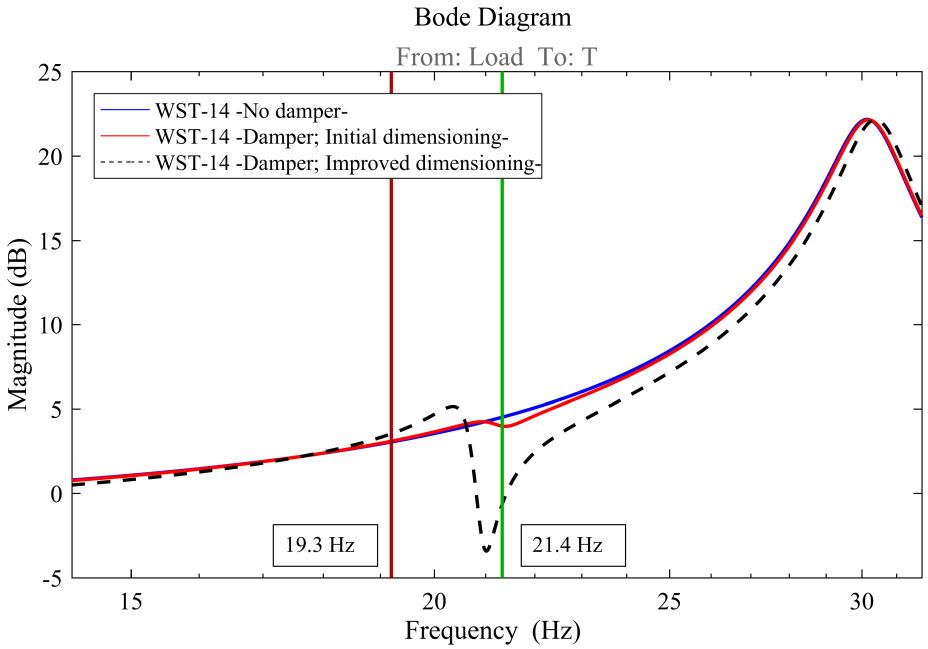

Figure 3.12. *Bode diagram of WST-14 simulation model with variable size passive ideal dampers*

It can be seen from the bode diagram that the initially dimensioned damper that would fit in to the WST-14 cone has negligible damping effect in the propeller shaft as there is very small difference in magnitude compared to a system without a damper.

This leads to a fact that a bigger damper must be dimensioned and parametrized. Differences between the initially dimensioned damper and an improved damper can be seen in Table 3.1. As it is determined that a rotational damper which would fit into the thruster's cone has negligible effect, the dimension constraints are the first ones relaxed, but dimensions are kept as small as possible.

Table 3.1. *Dimensions and coefficients of passive ideal dampers*

	Initial damper	**Improved damper**
Material	Steel	Tungsten
Diameter [mm]	600	800
Length - case [mm]	50	70
Length - wheel [mm]	150	160
Inertia - case [kgm^2]	5	55
Inertia - wheel [kgm^2]	15	126
Weight - case [kg]	100	647
Weight - wheel [kg]	340	1 580
Spring coeff. K [kNm/rad]	270	2 280
Damping ratio ζ [%]	2	1
Damping coeff. C [Nms/rad]	80.4	339

As the two passive ideal dampers are compared, few major points must be noted. The material has been changed to tungsten that is approximately three times as dense as steel. This is done in order to increase the inertia as well as keep the damper's size as small as possible. The change in the material as well as making the damper 33 % larger in diameter, both inertia and weight increase heavily. Inertia and weight of the damper case are increased by 1 000 % and 550 %, respectively. Damper wheel's inertia and weight are increased by 740 % and 360 %, respectively. There is also a major change in the spring coefficient as it increases relatively as much as inertia. Same happens with the damping coefficient but the change in the damping ratio mitigates the effect to half.

Bode diagram of a passive ideal damper also shows the main problem with the damper. If a passive damper is tuned to the propeller blade frequency of 21.4 Hz the damper will only reduce torque peaks that occur at or extremely near said frequency. Passive damper does not have any noticeable effect if rotational speed of the propeller shaft is below 320 rpm, that is if the thruster is not driven at full speed. Ice impacts may also alter the rotational speed of the propeller shaft and thus lower the propeller blade frequency. It is estimated that maximum drop in frequency could be as high as 10 %. This is especially problematic with a passive damper as the damper could actually increase the torque amplitude of an ice impact as it can be deduced from the bode diagram.

Next step is to parametrize the hydraulic-mechanical damper. Tuning the hydraulic-mechanical damper is done with the help of simplified Simulink model of an ice impact scenario. Sinusoidal relative angle and angular velocity is input to models of hydraulic spring element and hydraulic damping element and the the resulting torque of this simplified simulation is compared and matched to an ideal system. As the hydraulic-mechanical damper is tuned, it is tested in the WST-14 model with ice impacts. Parameters of a tuned hydraulic-mechanical damper are shown in Table 3.2.

Table 3.2. *Parameters of hydraulic-mechanical damper*

Parameter	**HM Damper**
Spring element location [mm]	300
Spring element piston radius [mm]	22
Spring element cylinder chamber length [mm]	85.2
Spring element initial pressure [bar]	100
Number of spring elements	2
Damping element location [mm]	300
Damping element piston radius [mm]	28.2
Damping element cylinder chamber length [mm]	20
Damping element initial pressure [bar]	10
Valve nominal flow [l/min]	60
Valve nominal pressure [bar]	5
Valve opening time [ms]	5
Valve rise time [ms]	1
Number of damping elements	2

With parameters shown in Table 3.2 the hydraulic-mechanical damper has very similar spring coefficient K_{hydr} to the ideally calculated spring constant K and slightly lower damping coefficient C_{hydr} compared to ideal damping constant C, assuming the valve is fully open. Locations of spring and damping elements are chosen so that the elements dimensioned fit inside the damper physically and are as far away as comfortably possible from the center of the rotating damper. This leads to more torque generation with components of same size. Locations of the elements can be changed if more suitable ones are found. Number of the spring and damping elements is chosen as two of each, but the number can be increased. Decreasing the number of the elements to one would lead to unbalanced rotating damper which would require auxiliary balancing elements.

Size of the whole spring element is determined by the piston radius and cylinder chamber length along with the actual metal casing of the cylinder. With two cylinder chambers and an approximation of a cylinder casing and piston the length of

the spring element is 200 mm. Diameter of the cylindrical spring element is approximated at 60 mm. The spring element increases in size if the auxiliary pistons are added to create an active or a semi-active hydraulic spring. Initial pressure is set to 100 bar on both chambers and the simulated maximum pressure in a chamber is at 170 bar and the minimum chamber pressure at 30 bar.

Size of the damping element can't be approximated as accurately as the spring element because the damping element contains valves and connecting hoses. Length of the damping element's cylinder is approximately 80 mm with piston and cylinder casing and diameter of the cylinder is approximately 70 mm. Size of the damping element increases as the valves and hoses are installed. Initial pressure of the damping element's chambers can be set lower compared to the spring element's chamber pressures. This is due to the operation principle of the damping element described in the section3.3.

Valve in the damping element has few key tunable parameters. The valve should be big enough that it does not caused too much pressure difference over the cylinder chambers as it is fully open. In a fully passive system the valve can be replaced by suitable constant orifice that constantly causes desired level of damping. If a controlled valve is chosen, the nominal flow of the valve should be at least 60 l/min at nominal pressure of 5 bar. Valve to control the fluid flow could be similar to a 2FRH16-3X/60L from Bosch Rexroth [2]. In active damping element the valve should be fast enough to open and close to achieve best possible damping effect, but this is a minor challenge compared to creating a system that is fast enough to detect ice impacts and control the valve. Opening time of the valve is set to 5 ms and rise time of the valve is set to 1 ms in the simulations as approximations.

4. SIMULATION RESULTS AND ANALYSIS

As the dimensioning and parametrization is completed sufficiently well the ice impact cases will be simulated and analyzed with the rotational dampers. Different kind of ice impact series with varying amplitudes, rotational speeds and hit lengths are all studied. Torque response of the propeller shaft is studied most intensely, but other important aspects of ice impact responses are observed.

Many different simulations are done for the systems to determine how the hydraulic-mechanical damper functions in different situations. Different ice impact cases are simulated and studied as well as the differences between passive ideal damper and hydraulic-mechanical damper. Both custom ice impact series and ice impact cases determined in DNV regulations [3] are simulated and studied.

Simulation results of multiple ice impacts are shown in Appendix B. First three ice impacts are similar to the cases 1 - 3 of DNV regulations [3], respectively. Ice impacts 4 - 8 are custom ice impacts with relative impact lengths ranging from 10 % to 90 % with 20 % interval. These simulations are conducted with rotational speed of 320 rpm of the propeller shaft. Effects on both propeller shaft rotational speed and torque can be seen as well as maximum and minimum torques of each case. Nominal torque of 38.8 kNm and the nominal rotational speed is marked to the figure as a red line. All of the impact series, except of the case 2 of the DNV regulations, are are shaped identically with 4 rising impacts, 8 full torque impacts and 4 receding impacts. Impact series 1 and 4 - 8 are with a 75 % nominal torque load, impact 2 is with 100 % and impact 3 is with 50 % torque load.

In the multiple ice impact Figure 1 of Appendix B it is noted that the impact case 1 of DNV regulations as well as similar impact series with 90 % relative length result in highest torque peaks. As the torque vibrates, lowest torque loads occur in a custom ice impact series with a 50 % relative length. Rotational speed of the propeller shaft changes only a maximum amount of 2 % and the highest drop in the rotational speed is in a case 2 of the DNV regulations and least change is in a 10 % relative length impact series. Changes in rotational speed are assumed to be larger in real ice impact situations as the thruster model takes only the ice impact torque

load into account.

4.1 Ice impact case 1 of DNV regulations

First ice impact simulations with a damper are done with the WST-14 propulsion system and both the ice impact generator as well as the hydraulic-mechanical damper connected. The first ice impact simulated is the case 1 of the DNV regulations that is shown in 2.8. In this simulation case the nominal torque load is 38.8 kNm with 1.5 kNm amplitude vibration from the motor, ice impact load is 75 % of the nominal load and the ice impact frequency is at four times the propeller shaft rotational frequency that is 21.33 Hz. Length of each blade hit is 90 ° so a new sinusoidal impact starts at the same instant the previous one ends.

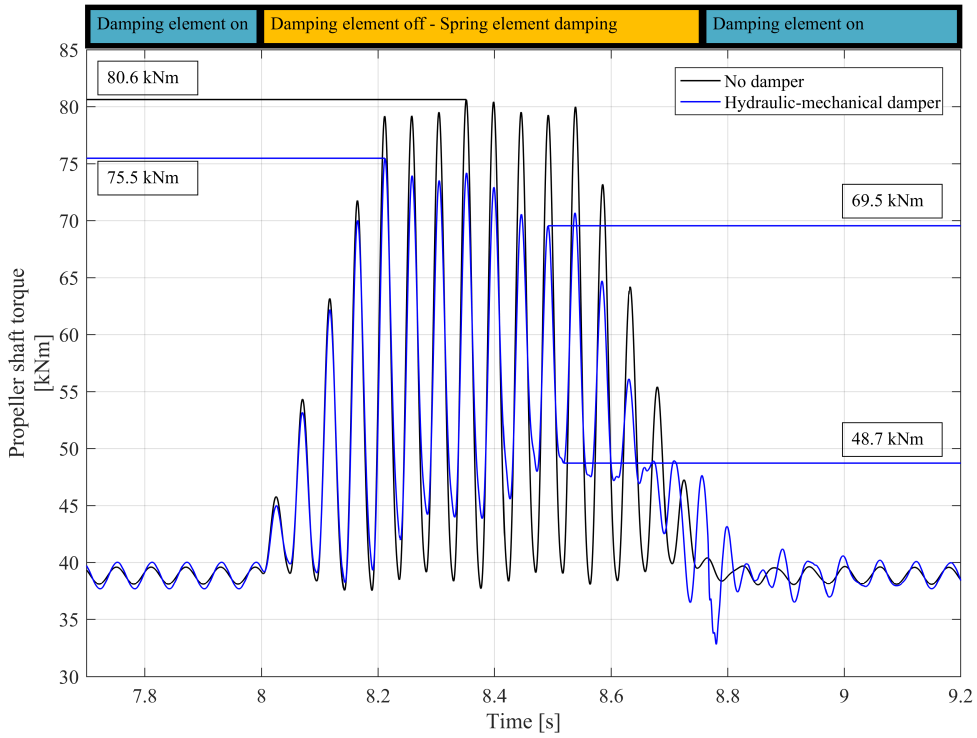

Figure 4.1. *Simulation results of DNV Case 1 impact with a hydraulic-mechanical damper - Propeller shaft torque*

As it can be seen from the Figure 4.1, the hydraulic-mechanical damper does have an effect on the torque of the propeller shaft caused by an ice impact. Without the damper the maximum torque peak is at 80.6 kNm and with the hydraulic-mechanical damper the maximum torque peak is at 75.5 kNm. This is roughly 6.3 % difference in the torque peak if it is calculated from the absolute zero. If the calculation is conducted from the nominal load of 38.8 kNm, the difference is 12.2 %. As the ice

impact similar to the case 1 of DNV regulations is a series of propeller blade hits to ice, it can be seen that if the impact lasts longer, the hydraulic spring of the HM damper has enough time to vibrate the wheel inertia more and thus it causes more torque reduction. Maximum peak reduction caused by the hydraulic-mechanical damper is approximately 10 kNm, so the maximum reduction in peak-to-peak torque is doubled. Peak-to-peak torque levels in a maximum damping situation are from 48.7 kNm to 69.5 kNm which is a peak-to-peak torque of 20.8 kNm. Without a damper at the same exact time the peak-to-peak torques are from 39.0 kNm to 79.3 kNm, a peak-to-peak torque of 40.3 kNm. This is a difference of 48.4 %.

In these simulations the hydraulic-mechanical damper is an active one. From the top of the Figure 4.1 it can be seen that the damping element is active when there is no ice impact ongoing. As the ice impact is detected, the damping element is switched off and the valve is opened. Damping element is activated and the valve is closed again as the ice impact recedes. Hydraulic spring element is semi-active so the damper is continuously tuned to ice impact frequency.

Noteworthy in the first simulation is also that with the damper the propeller shaft torque keeps vibrating after the ice impact. This is due to the hydraulic spring generating torque with the inertia wheel even after the impact. This vibration is mitigated fast by activating the hydraulic damping element. Also the amplitude of the vibration before and after the ice impact is slightly larger with the damper. This is due to the extra inertia of the damper.

Passive ideal damper is simulated as a reference point. The hydraulic-mechanical damper is dimensioned and parametrized after the passive ideal damper so in an ideal situation where both dampers are tuned properly to the ice impacts, the difference between the two should be minimal. In situations where the active hydraulic damping element is active, the difference between the dampers is considerable. Difference can be observed in Figure 4.2.

In the plot 4.2 y-axis is the torque the damper generates to the propulsion system. After the damping element is activated, the torque generated by the hydraulic-mechanical damper falls quickly when the passive ideal damper keeps on vibrating with higher amplitude. The slight difference in the start of the ice impact phase in damping torque is caused mostly by the friction of the non-ideal hydraulic-mechanical damper.

Next simulation is about the same ice impact case 1 of the DNV regulations, but thruster is not driven with the nominal speed of 320 rpm but with 8 % lower rotational speed of 295 rpm. Semi-active spring of the hydraulic-mechanical damper is

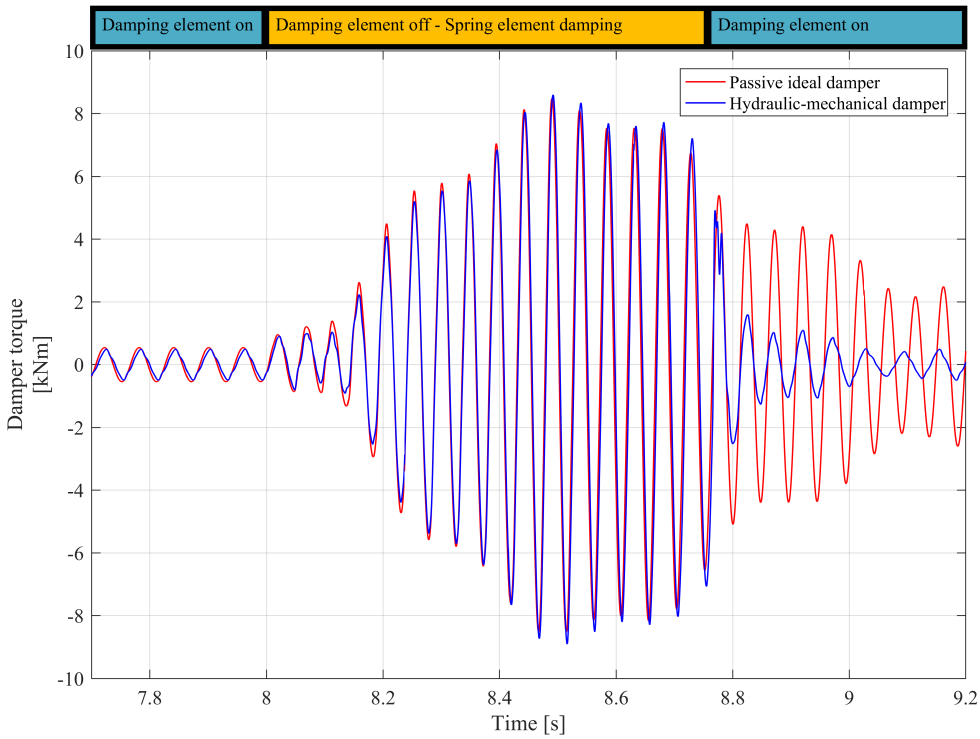

Figure 4.2. *Simulation results of DNV Case 1 impact with a hydraulic-mechanical damper - Damper torque*

automatically tuned to the altered rotational speed, but the passive ideal damper is not. Passive ideal damper even increases the propeller shaft torque, as it is shown in the magnitude plot of the bode diagram in Figure 3.12, with this rotational speed of the propeller shaft. The simulated propeller shaft torques can be seen in Figure 4.3.

Torque of the propeller shaft without the damper and with the active hydraulic-mechanical damper can be seen in the top plot of Figure 4.3. Lower plot shows the torque without the damper and with the passive ideal damper. With altered rotational speed the hydraulic-mechanical damper works similarly to the first simulation lowering the torque peaks and peak-to-peak torque. Passive ideal damper on the other hand slightly increases torque peaks and peak-to-peak torques and longer the impact series lasts, more the increase. In this case the torque peak increase is roughly 3 %.

Simulation studies of the system including relative angle, angular velocity and propeller shaft rotational speed can be seen in Appendix C Figure 2. System is simulated with the hydraulic-mechanical damper. In the plot we can see the change in rotational speed of the propeller shaft which is 4 rpm or roughly 1.25 %. In this ice

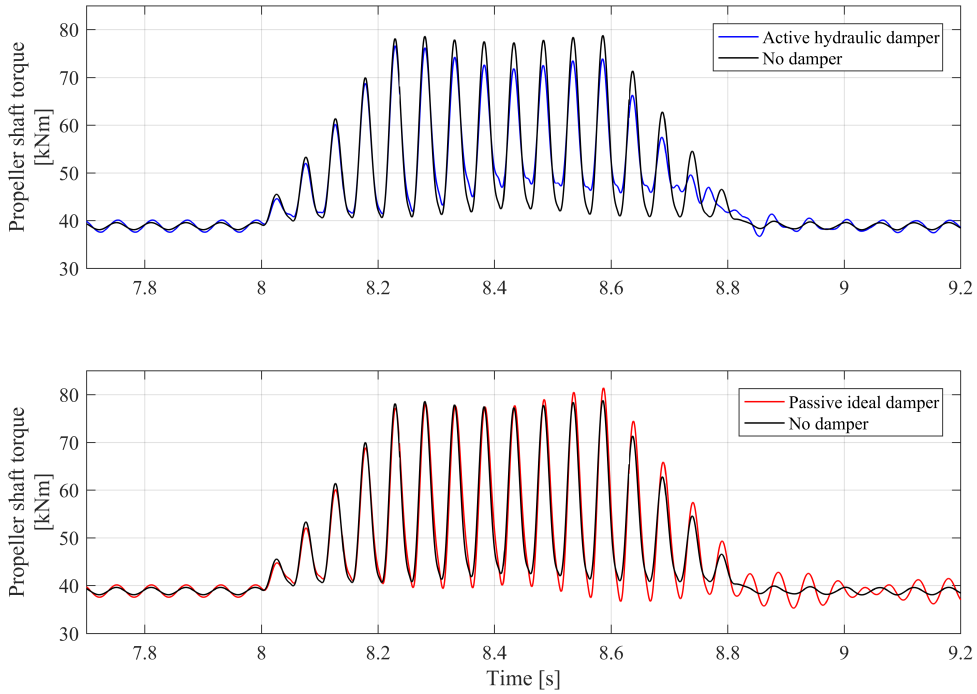

Figure 4.3. *Simulation results of DNV Case 1 impact with a hydraulic-mechanical damper - Non-nominal speed*

impact case drop in the rotational speed is far from the assumed maximum of 10 %, but even a change this small has effect on a passive ideal damper as the propeller blade frequency changes.

Relative angle of the damper case and wheel oscillates with an amplitude of 4.5 mrad and relative angular velocity oscillates with an amplitude of 0.5 rad/s. Relative angle between the damper case and wheel is small as the frequency of the oscillation in the system is relatively high. Amplitude of 4.5 mrad oscillation translates to 0.258° and 1.8 mm of relative displacement in the outer edge of the damper. Small relative displacement leads to problems with damper systems as the damper must be constructed with low tolerances to function well with small displacements and angles.

4.2 Ice impact case 2 of DNV regulations

Next simulation case is similar to the case 2 of the DNV regulations. Simulations are again conducted without the damper, with the hydraulic-mechanical damper and with the passive ideal damper. Torque load of the ice impact case 2 is 100 % of the 38.8 kNm nominal load so the load peaks are at 77.6 kNm. Individual impacts

to the propeller blade are 135° long and occur every 90°. Response on the propeller shaft is seen in Figure 4.4.

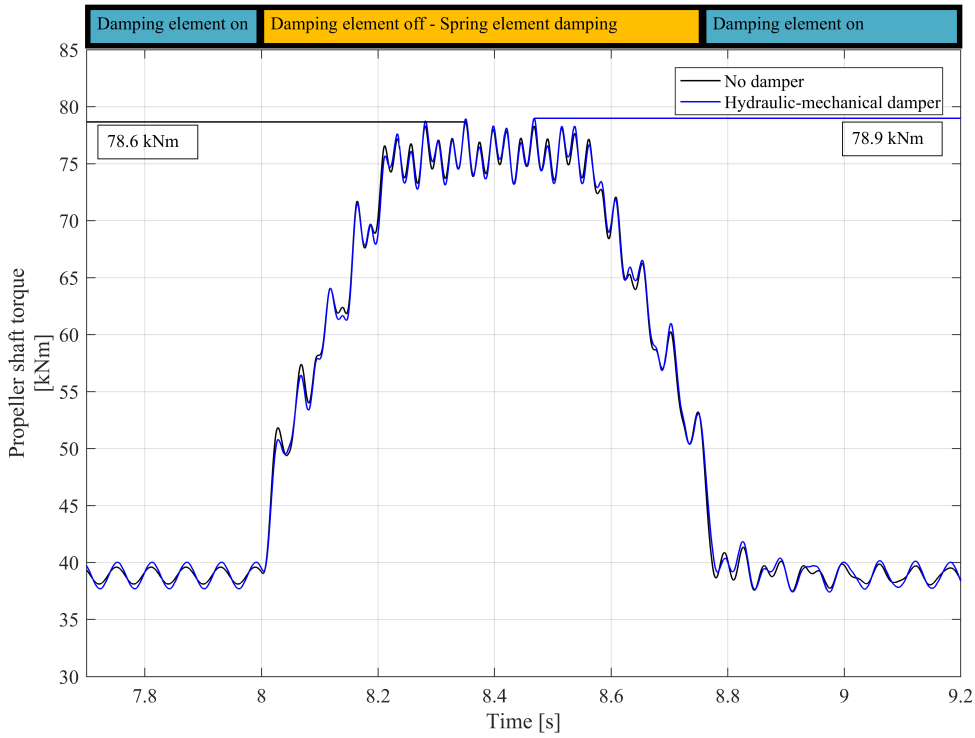

Figure 4.4. *Simulation results of DNV Case 2 impact with a hydraulic-mechanical damperd*

As it can be seen from the torque response, hydraulic-mechanical damper does not reduce torque in this case, but increases the peaks torque slightly. In this case the hydraulic-mechanical damper and a passive ideal damper have identical results except for the residual vibrations that are reduced by the active hydraulic-mechanical damper. Maximum torque peaks in the propeller shaft in this impact case are 78.6 kNm without a damper and 78.9 kNm with the hydraulic-mechanical damper. Increase in the maximum torque peak is 0.3 kNm that is roughly 0.4 % of an absolute increase. This is unwanted behavior, but can't be helped with a spring-mass type damper.

Fact that a rotational damper does not reduce torque in this impact case is due to damper design. Torque reduction of a rotational damper occurs because of the vibrations caused by a tuned spring. In this impact case the torque of the propeller shaft does not vibrate but rather steadily rises to higher level, rotational damper can't vibrate and reduce the torque. Damping this kind of an impact would require a motor- or a brake-type damping system that would decrease the torque peaks.

Propeller shaft rotational velocity response can be seen in the Figure 1 of Appendix B. Impact case 2 results in biggest drop in the rotational velocity of all of the simulated cases as it was expected and the difference in the velocity drop is over 20 %. In a realistic situation the rotational speed would most likely fall even more. Damping impacts such as the case 2 of DNV regulations would be extremely helpful as these impacts are often caused by bigger ice blocks. Big ice blocks can also cause the propeller to get stuck on to ice.

4.3 Ice impact case 3 of DNV regulations

Case 3 of the DNV regulations is similar to the case 1 except the ice impacts occur at a double frequency. With a nominal propeller shaft rotational speed of 320 rpm, the frequency in ice impact case 3 is approximately 42.66 Hz. Propeller blade hits ice every 45° and an impact lasts for 45°. This kind of an impact case would require two ice blocks being hit and rotated by the thruster's propeller blades. Torque load of said impact series is 50 % of the nominal load. Propeller shaft torque response is plotted in Figure 4.5.

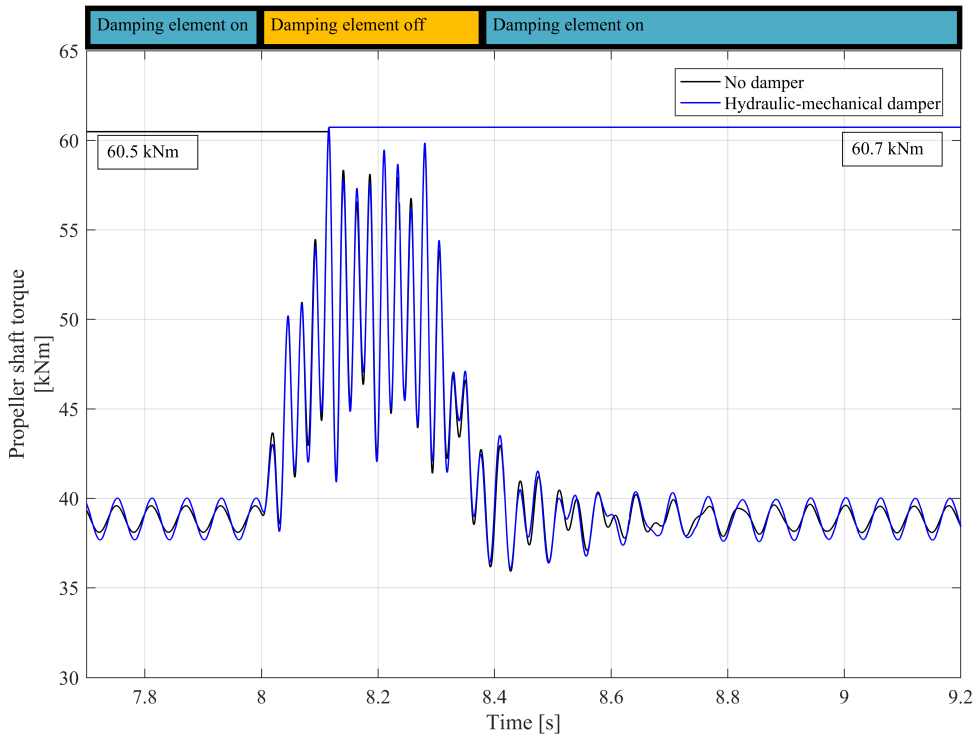

Figure 4.5. *Simulation results of DNV Case 3 impact with a hydraulic-mechanical damperd*

Without a damper the case 3 of the DNV regulations is the mildest impact case.

Compared to the two other cases, ice impact case 3 has smallest torque peaks. Increases in torque peaks are only roughly 50 % compared to the first case. Similar response can be seen in the rotational speed. Maximum drop in the rotational speed is roughly 40 % smaller than in the case 2 which has the largest rotational speed reduction peaks.

In the impact case 3 a rotational damper practically has no effect on the torque response as the damper is tuned to incorrect frequency. Even the semi-active hydraulic spring element does not have an effect as the change in frequency is not related to the rotational speed but rather to the ice blocks the propeller blades are hitting. As it can be seen in Figure 4.5 the damper increases the torque peaks due to the increased total inertia of the system. Increase in the torque peaks is 0.2 kNm or 0.3 % and thus it is almost negligible.

4.4 Custom ice impact series

Next simulations are done with a custom ice impact profile. One of the important functions of a damper is to prevent the torque of the propeller shaft to fall under zero causing gear hammering. Next ice impact is generated with custom mode with a sinusoidal impact of 50 % relative length and 60 kNm torque load that is approximately 155 % of the nominal load. Total load torque peaks are 98.8 kNm. This kind of an ice impact profile is most likely to cause negative torques as the ice impact occurs every 45° of propeller shaft rotations and there is a 45° gap before next impact starts. Torque response of the propeller shaft can be seen in Figure 4.6.

From the Figure 4.6 it can be observed that without a damper the propeller shaft torque falls to zero. Absolute torque would fall below zero, but the simulation model can't handle torques below zero. In theory after this kind of a situation the simulation results are no longer perfectly valid after hitting the zero torque, but simulation functions as an approximation. As the ice impact load profile is different, the propeller shaft torque changes. Maximum peak of the propeller shaft torque is above 100 kNm and the minimum would theoretically be close to -2 kNm.

With the hydraulic-mechanical damper the torque does not fall near zero at all and stays at a minimum of 7 kNm. In this case the hydraulic-mechanical damper prevents the gear hammering. Maximum peak torque with the damper in a custom ice impact series is 95 kNm so the propeller shaft torque is reduced. In this kind of a situation where the ice impacts are generated at the nominal rotational speed of the propeller shaft, the passive ideal damper would have almost identical effect on the torque.

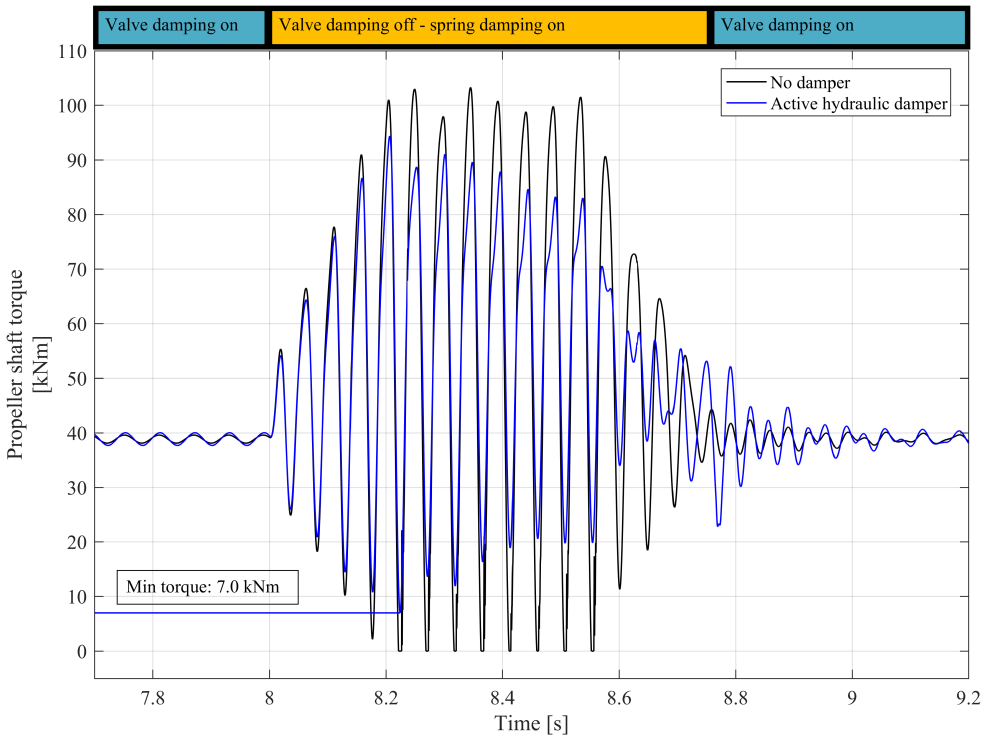

Figure 4.6. *Simulation results of custom ice impact case - gear hammering, 50 % relative length and bigger torque load*

Last simulations are conducted with different relative ice impact lengths. All of the simulations are done with identical parameters, except for the difference in relative length. Rotational speed of the propeller shaft is set at the nominal 320 rpm, torque load is the nominal load of 38.8 kNm and ice impact loads are 75 % of the nominal. Simulation are done with 25 %, 50 % and 75 % relative lengths to study the functionality of the hydraulic-mechanical damper in these situations. Torque and velocity responses of several other custom ice impact cases can be seen in Figure 1 Appendix B.

In the first simulation case of ice impact series with 25 % relative length is shown in Figure 4.7. Relative length 25 % translates to 22.5° long sinusoidal impact and a 67.5° break. From the simulation it is noted that in this custom case the damper does reduce the torque peaks, but not efficiently. Reduction is only 0.3 kNm or 0.5 % calculated from the zero torque. Reduction of the falling torque peaks is more significant, from 23.1 kNm to 26.3 kNm. Falling torque reduction is 3.2 kNm that is roughly 20.4 % from the nominal torque of 38.8 kNm.

In the case of 25 % relative length, it can be observed that even as the ice impact load torque stays at constant 75 % of the nominal load, the torque peaks are lower

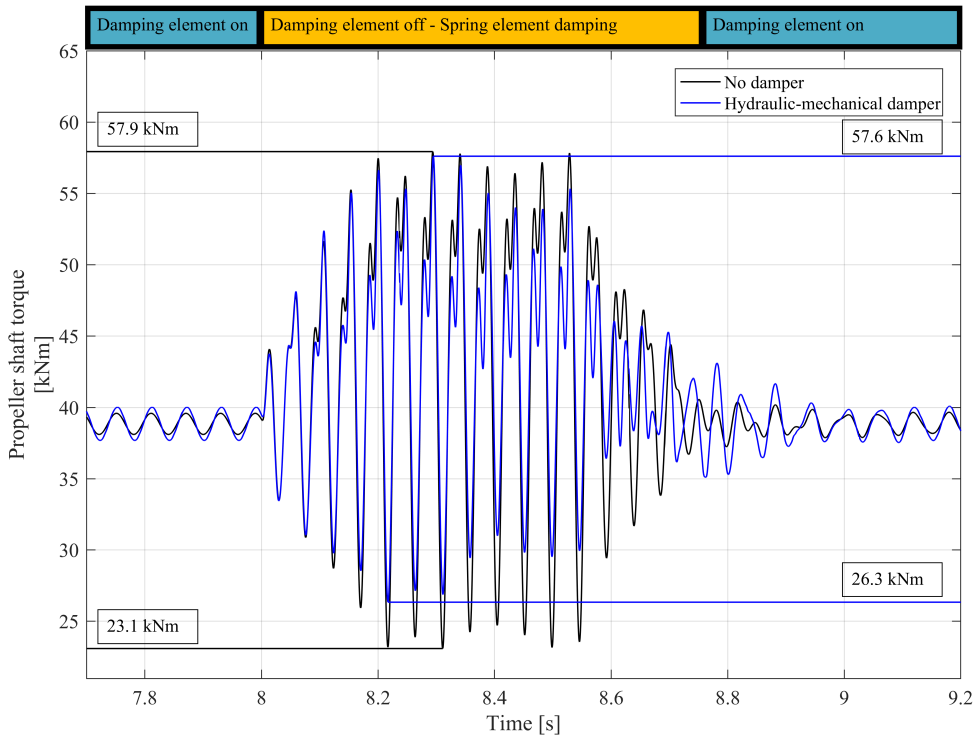

Figure 4.7. *Simulation results of custom ice impact case - 25 % relative length*

than e.g. in the case 1 of the DNV regulations. Also the shape of the propeller shaft torque response has additional peaks and slopes. Additional peaks are assumed to occur because of the nominal frequencies of the propeller shaft and because the 25 % impact oscillates the propeller shaft with virtually doubled frequency.

Next simulation is with the same relative length of 50 % as the gear hammering simulation. In this simulation the ice impact torque load is kept at the nominal 75 %. Simulation results can be seen in Figure 4.8. It can be seen that the propeller shaft torque response is closer to proper sinusoidal wave compared to the previous simulation. Torque response without the damper is very close to perfect sinusoidal wave, but system with the damper has some irregularities still. This is assumed to be due to the extra inertia of the damper.

Torque peak reduction in the 50 % relative length impact case is from 69.5 kNm to 65.7 kNm. Peak torque reduction in this case is 3.8 kNm or 5.5 %. Falling peak torque reduction is again more significant, 5.6 kNm or 27 % calculated from the nominal torque of 38.8 kNm.

The final simulation is conducted with an ice impact series of 75 % relative length and otherwise identical conditions to the two previous simulations. Torque response

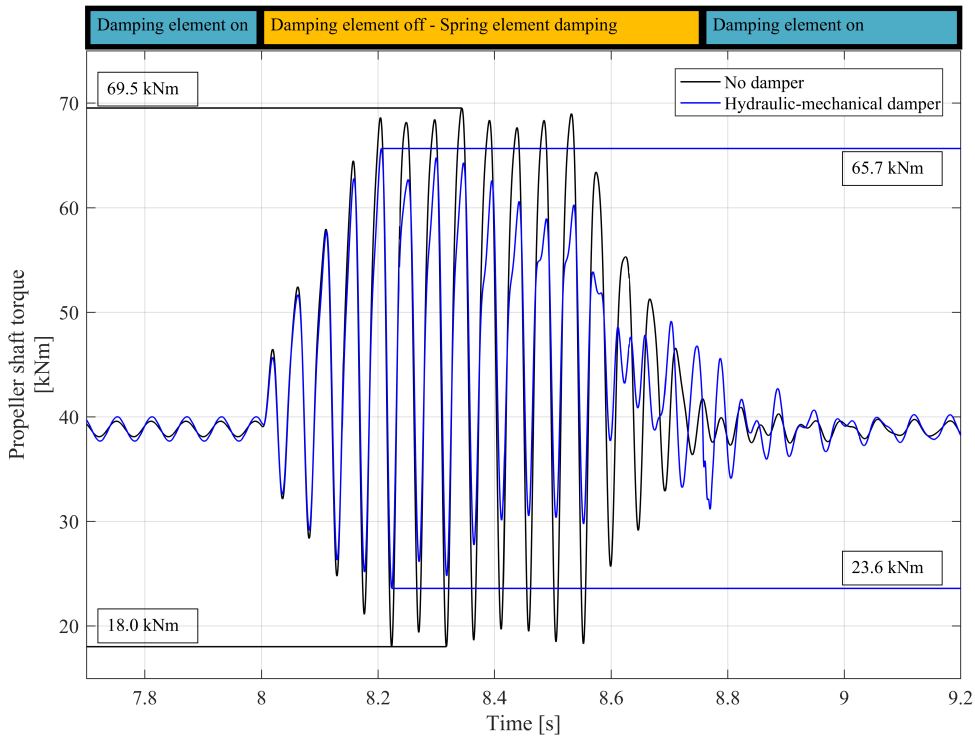

Figure 4.8. *Simulation results of custom ice impact case - 50 % relative length*

of this simulation can be seen in Figure 4.9. It can be seen that as the relative length of the impact gets lengthens so does the maximum torque peak. Also the peak torque damping increases. Peak torque is reduced from 80.3 kNm to a 73.4 kNm with the hydraulic-mechanical damper. Torque peak reduction is 6.9 kNm or 8.6 % from the zero torque. Falling torque is reduced from 25.5 kNm to 30.6 kNm, that is 5.1 kNm or 38.4 % calculated from the nominal torque.

The three previous simulations show that the longer relative length of the impact is, the more peak torque reduction is achieved with the damper. Longer relative length also means a higher peak torque and this leads to the fact that a functioning damper is more important.

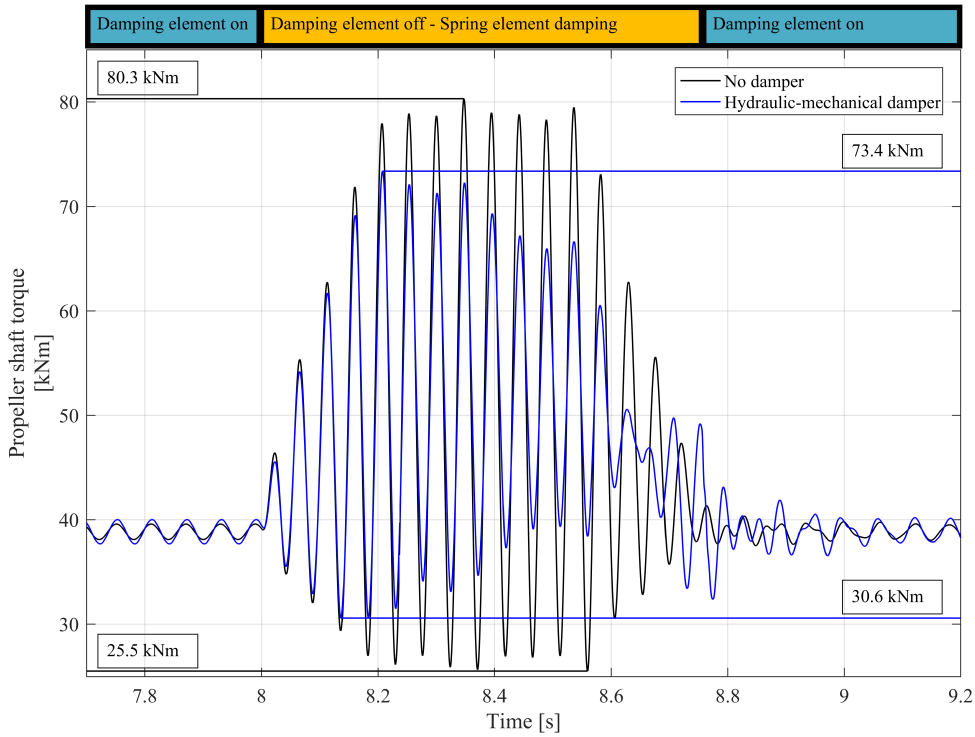

Figure 4.9. *Simulation results of custom ice impact case - 75 % relative length*

5. CONCLUSIONS AND DISCUSSION

This master's thesis consisted of designing and modelling a damper system for a Wärtsilä Steerable Thruster. Aim of the thesis was to reduce torque peaks caused by ice impacts on the propeller shaft of the thruster. Current commercial dampers were studied in a literature review part and it was decided that the commercial dampers are not suitable for the project and a novel damper should be designed. A passive ideal damper as well as a novel hydraulic-mechanical damper were modelled and dampers' effects were simulated in varied ice impact scenarios.

Simulated ice impact cases were generated to be similar to the ones of DNV regulations as well as additional custom ice impacts with different sinusoidal impact lengths. Simulations were conducted without a damper, with a passive ideal damper and the designed novel hydraulic-mechanical damper. A validated simulation model of a WST-14 propulsion system was given for this master's thesis by AUT laboratory.

Designed novel hydraulic-mechanical damper is a rotational dual-mass torsional damper. Damper consists of two main inertias; a damper case and a damper wheel, as well as hydraulic spring and damping elements. Both active and semi-active variations of the damper are considered. Brief summary of the simulation results can be seen in next section.

5.1 Summary of hydraulic-mechanical damper simulations

Main simulation results of the hydraulic-mechanical damper are clear. Designed damper does function in certain common impact cases as the damper reduces the torque peaks caused by ice impacts. In certain cases damper will have negligible or even inverse effect. Short summary of the hydraulic-mechanical damper's overall performance estimation as well as peak torque reduction can be seen in Table 5.1.

Hydraulic-mechanical damper causes notable reduction in torque peaks in ice impact case 1 of the DNV regulations as well as custom impact cases with longer than 50 % relative length. In custom ice impact cases of differing relative length the falling torque reduction is 20 - 40 %. This means that in these cases the damper could

Table 5.1. *Summary of the hydraulic-mechanical damper*

Ice impact shape	Overall performance estimation	Torque peak reduction
Case 1 of DNV	Average	-6.3 %
Case 2 of DNV	Inverse - Bad	+0.4 %
Case 3 of DNV	Inverse - Bad	+0.3 %
25 % relative length	Minor	-0.5 %
50 % relative length	Average	-5.5 %
75 % relative length	Good	-8.6 %
Gear hammering	Good	-

prevent gear hammering. Peak-to-peak reduction in certain cases is significant, over 40 % in best case scenarios. In impact cases 2 and 3 of the DNV regulations the hydraulic-mechanical damper acts inversely and increases the propeller shaft torque but by a very small amount.

Hydraulic-mechanical damper functions very similarly to a passive ideal damper as the hydraulic-mechanical damper is tuned accurately with the help of ideal coefficients. Active damping element of the hydraulic-mechanical damper reduces the excess vibration after impacts contrary to a passive ideal damper. Also semi-active spring element improves the hydraulic-mechanical damper compared to a passive ideal one. Semi-active spring element keeps the hydraulic-mechanical tuned even if the rotational speed of the propeller shaft varies.

5.2 Future research

It is stated in this thesis that the simulated novel hydraulic-mechanical damper does work but not very efficiently. Some improvisations could be made for the design of the damper. Damper can be made more active and thus more effective. One concept to make the damper reduce the torque peaks more is to include a preloaded spring that is activated as an ice impact is detected. This design would make the damper reduce the torque peaks with maximum efficiency right as the impact series starts. Also a fully active control of the spring coefficient is possible and this would allow damper to be tuned on different impact frequencies.

Improvement methods mentioned require an effective and fast controller as well as a good method to detect the ice impacts. Especially a method to detect the ice impacts effectively is one crucial research topic as the active damping element of the hydraulic-mechanical damper already requires detection of the impacts.

After the improvements a proper realizable design of the hydraulic-mechanical damper could be created. This would include e.g. accurate dimensioning, detailed CAD models, bearings and the attachment to the propeller shaft. Additionally the hydraulic-mechanical damper could be made easier to manufacture with different materials, dimensions or altered spring and damping elements.

BIBLIOGRAPHY

[1] ABB, "Azipod C Propulsion and Thruster units for 1300 - 4500 kW," 2015, Available: https://library.e.abb.com/public/3fcd7b9606275fe5c1257a3300279df1/Azipod_C_Presentation.pdf, accessed 4/2017.

[2] Bosch Rexroth AG, "2-way flow control valve," Available: https://dc-us.resource.bosch.com/media/us/products_13/product_groups_1/industrial_hydraulics_5/pdfs_4/re28163.pdf, accessed 4/2017.

[3] DNV, "Ships for navigation in ice," Jul 2011, part 5 chapter 1, 141 p. Available: https://rules.dnvgl.com/docs/pdf/DNV/rulesship/2011-07/ts501.pdf, accessed 2/2017.

[4] Geislinger, "Damper catalogue," 2015, Available: http://www.geislinger.com/assets/geislinger.at/downloads/Damper_15.7new.pdf, accessed 10/2016.

[5] Geislinger, "products, customized steel spring damper," 2015, Available: http://www.geislinger.com/en/products/product/damper, accessed 10/2016.

[6] Geislinger, "products, vdamp," 2016, Available: http://www.geislinger.com/en/products/product/vdamp, accessed 10/2016.

[7] Geislinger, "Vdamp, catalogue," 2016, Available: http://www.geislinger.com/assets/geislinger.at//downloads/Vdamp_1.4.pdf, accessed 10/2016.

[8] Hasse & Wrede, "Hydraulic dampers," 2016, Available: http://www.hassewrede.de/en/produkte/hydraulischedmpfer/hydraulischedmpfer_1.jsp, accessed 10/2016.

[9] Hasse & Wrede, "Hydrolastic - damper," 2016, Available: http://www.knorr-bremse.de/en/commercialvehicles/products_1/dampres/dampers.jsp, accessed 10/2016.

[10] Hasse & Wrede, "Torsional visco-dampers," 2016, Available: http://www.hassewrede.de/en/produkte/viscodmpfer/viscodmpfer_1.jsp, accessed 10/2016.

[11] Hasse & Wrede, "Visco damper," 2016, Available: http://www.hassewrede.de/media/documents/Serviceflyer.pdf, accessed 10/2016.

[12] Hasse & Wrede, "Visco-dampers, designs," 2016, Available: http://www.hassewrede.de/en/produkte/viscodmpfer/designs/designs_1.jsp, accessed 10/2016.

[13] T. Ikonen, O. Peltokorpi, and J. Karhunen, "Inverse ice-induced moment determination on the propeller of an ice-going vessel," *Journal of Cold Regions Science and Technology*, vol. 112, 2015, pp. 1-13.

[14] P. Koskinen and M. Jussila, "Potkurin lavan jääkuormien pitkäaikaismittaus m/s Gudingenilla," VTT publication 1260, Espoo, Finland, 1991, 46 p.

[15] M. Linjama, "Iha-2600 hydraulijärjestelmien mallinnus ja simulointi," Lecture material, TUT, AUT, 2006.

[16] M. MackAldener, "Tooth interior fatigue fracture & robustness of gears," Dissertation, Department of Machine Design, Royal Institute of Technology, Stockholm, Sweden, 2001, 49 p.

[17] MathWorks, "Model and simulate multidomain physical systems," 2017, Available: https://se.mathworks.com/products/simscape.html, accessed 4/2017.

[18] O. Peltokorpi, "Akselin jännitysten mittaus ja jääkuormitusten simulointi," Master's thesis, University of Oulu, Department of Mechanical Engineering, 2015, 70 p.

[19] S. Persson, "Ice impact simulation of propulsion machinery," *MTZ Industrial journal*, Mar. 2015, pp. 34-40.

[20] S. S. Rao, *Mechanical vibrations, 3rd edition.* Reading (MA), Addison-wesley Publishing, 1995, 912 p.

[21] M. Savolainen and A. Lehtovaara, "An experimental approach for investigating scuffing initiation due to overload cycles with a twin-disc test device," *Tribology International*, vol. 109, 2017, pp. 311-318.

[22] W. T. Thomson, *Theory of Vibration with Applications.* London, Unwin Hyman, 1989, 467 p.

[23] Trafi, "Ice class regulations 2010 "finnish-swedish ice class rules 2010"," Nov. 2010, 48 p. Available: https://www.trafi.fi/filebank/a/1328276403/5e67a19cb56529f0fbd531539e08438f/9131-36441-Jaaluokkamaaraykset_TRAFI_31298_03_04_01_00_2010_EN_corr_20_Dec_2010.pdf, accessed 2/2017.

[24] Voith, "Controlling forces. vibration damper hydrodamp," 2014, Available: http://resource.voith.com/vt/publications/downloads/58_e_g_1098_en_hydrodamp_2014-10.pdf, accessed 10/2016.

[25] Vulkan Couplings, "Explanation, explanation of technical data," 2016, Available: http://www.vulkan.com/en-us/couplings/Documents/Technische-Datenbroschueren-original/technical_data_explanation_082016.pdf, accessed 10/2016.

[26] Vulkan Couplings, "Rato ds, technical data," 2016, Available: http://www.vulkan.com/en-us/couplings/Documents/Technische-Datenbroschueren-original/technical_data_ratods_082016.pdf, accessed 10/2016.

[27] Wärtsilä, "Turn this way," 2016, Available: http://www.wartsila.com/resources/article/turn-this-way, accessed 10/2016.

[28] ZF MARINE KRIMPEN, "Commercial craft thruster systems," 2014, Available: https://www.zf.com/corporate/media/corporate_6/products/product_range/non_automotive/marine/marine_1/products_6/Commercial_Craft_Thruster_Systems_2014_EN.pdf, accessed 4/2017.

[29] ZF Sachs, "Experiencing dynamics - reliably," 2016, Available: https://ci-portal.zf.com/global/media/en_de/zf_media/document/corporate_2/downloads_1/flyer_and_brochures/commercial_vehicle_flyer/zf_bro_tn_2014_en.pdf, accessed 10/2016.

[30] ZF Sachs, "Zf technology in commercial vehicles, driveline components," 2016, Available: http://www.zf.com/corporate/en_de/products/product_range/commercial_vehicles/trucks_dynadamp.shtml, accessed 10/2016.

APPENDIX A. COMMERCIAL DAMPER SUMMARY

Table 2. *Summary of the commercial dampers*

	Pros	**Cons**
Voith Hydrodamp	-Wear free damping -Easily tunable damping effect & backlash -Easily made active with valves or MR/ER fluids	-Low maximum engine torque -Installation between engine and transmission -Normally not used in marine applications
Geislinger Damper	-Installment on propeller shaft is possible -Already used in marine environment -Wear free damping -Relatively small & low weight -May be customizable by differing oil pressures	-Requires supply of pressurized oil -May not be easy to customize and change active with valves e.g.
Hasse&Wrede Hydrolastic Damper	-Most likely scalable to marine applications -Long lifetime and long service intervals -Modification might be possible with MR/ER fluid or even some sort of a valve system / pressure	-Maximum engine power only 1,25MW according to catalogues. (Enough if installed elsewhere than straight to Engine?) -Not enough specifics and information available
ZF Sachs DynaDamp	-Easy to integrate to wide range of drive shafts	-Only used in construction machinery & trucks -Only 3.2kNm max torque -Not much information available
Geislinger Vdamp	-Already used in marine environment -Highly scalable (300mm to 4 000mm) -Modification might be possible with MR/ER fluid -Vdamp XT doubles fluid lifetime	-Viscous damping -> Wearing of the fluid -Viscous fluid must be changed from time to time
Hasse&Wrede Torsional Visco-damper	-Already used in marine environment -Off-the-shelf for 80MW engines	-Viscous damping -> Wearing of the fluid -Viscous fluid must be changed from time to time -Not enough information available
Vulkan RATO DS	-Used in marine applications and icebreakers -Max 160kNm torque	-Decoupling -> Constant losses -Malfunctions could result in to whole thruster stopping

APPENDIX B. MULTIPLE ICE IMPACTS

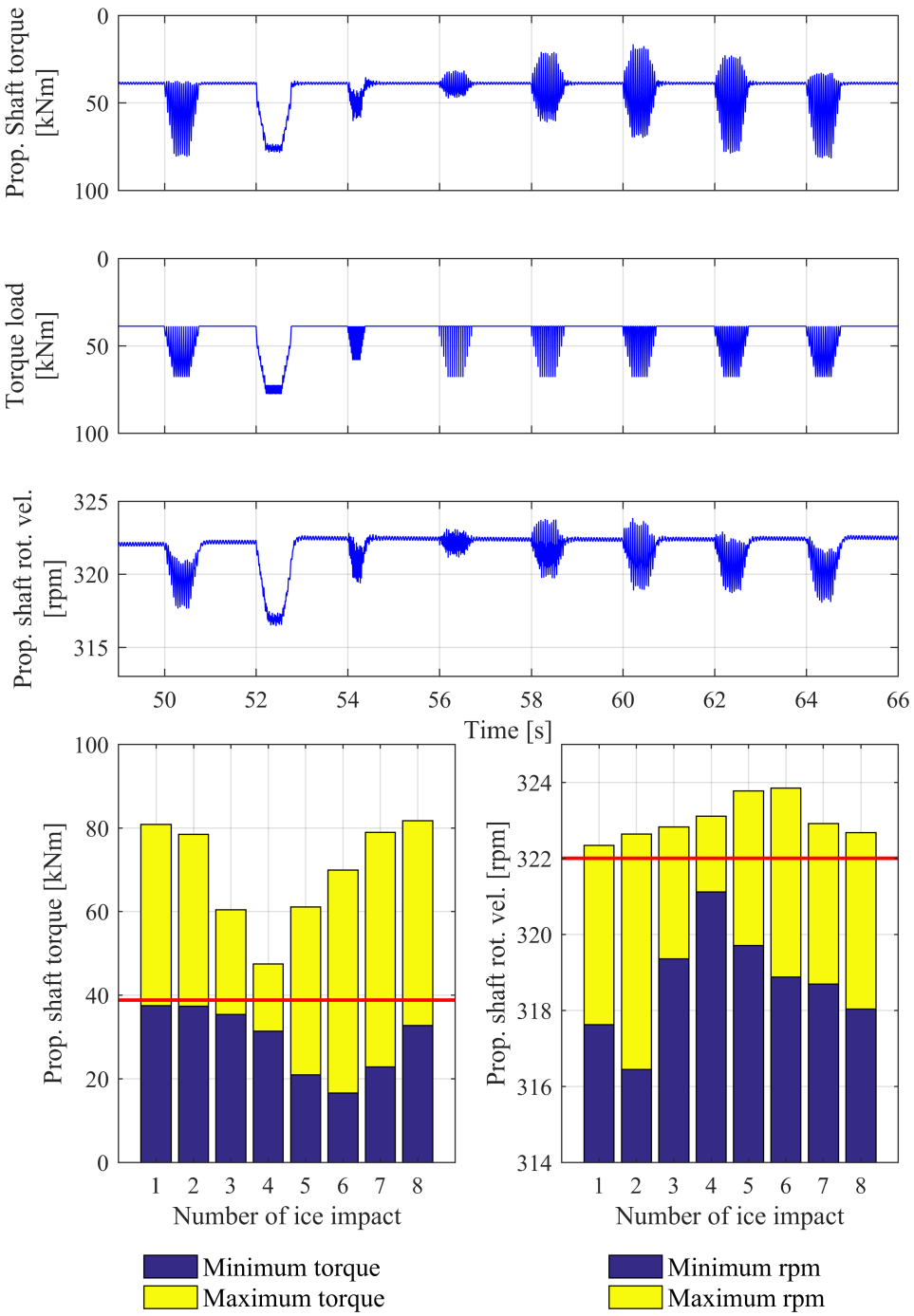

Figure 1. *Multiple ice impacts without a damper*

APPENDIX C. SIMULATION RESULTS OF IMPACT CASE 1

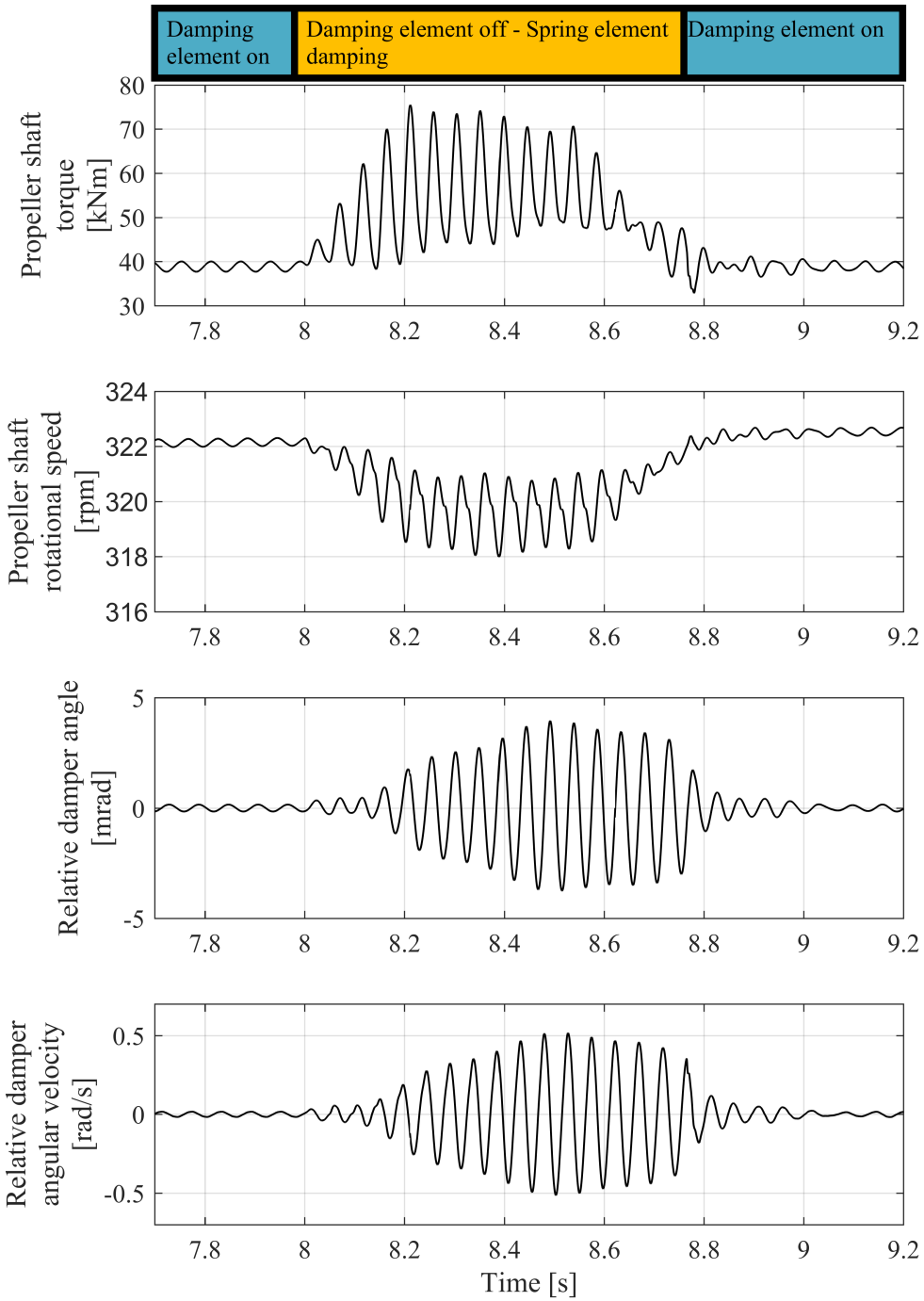

Figure 2. *Simulation results of impact case 1 with damper angle and angular velocity*